Türkiye Jeoloji Bülteni
Geological Bulletin of Turkey
68 (2025) 287–332
doi: 10.25288/tjb.1603626

Evolution of Neogene Sedimentary Rocks on the Southern Margin of the Alaşehir Graben: Evidence for Termination of Tectonic Activity on the Alaşehir Detachment Fault During the Late Miocene

Alaşehir Grabeni'nin Güney Kenarındaki Neojen Tortul Kayaçlarının Evrimi: Alaşehir Sıyrılma Fayının Tektonik Aktivitesinin Geç Miyosen'de Sona Erdiğine Dair Kanıt

Fatih Şen[1,2*], Serdal Karaağaç[1]

[1] *Fen Bilimleri Ensitüsü, İstanbul Üniversitesi, TR34116 Fatih, İstanbul, TÜRKİYE*
[2] *Department of Geological Sciences, University of Alabama, AL 35487-0338, Tuscaloosa, USA*

• Geliş/Received: 18.12.2024 • Düzeltilmiş Metin Geliş/Revised Manuscript Received: 12.04.2024 • Kabul/Accepted: 20.04.2024
• Çevrimiçi Yayın/Available online: 11.06.2025 • Baskı/Printed:
Araştırma Makalesi/Research Article *Türkiye Jeol. Bül. / Geol. Bull. Turkey*

Abstract: The southern margin of the Alaşehir Graben is bounded by the Alaşehir Detachment Fault (ADF), comprising ductile-brittle cataclastic rocks within the same extensional regime. This fault surface is exposed over ~150 km from Turgutlu to Alaşehir and dips to the north at a low-angle (10°-30°). There are two main interpretations about the termination of tectonic activity on the ADF. The first is that recent movement of the fault ended in the late Miocene, based on the fact that it is cut by Plio-Quaternary high-angle normal faults. The second view suggests that tectonic activity continued until the Plio-Quaternary, based on the exhumation ages obtained from cataclastic rocks. We present measured stratigraphic logs of the Neogene sequence in the hanging wall of the ADF in the Salihli and Alaşehir areas to contribute to this discussion. The depositional evolution of the Alaşehir Graben can be described in three assemblages, including Miocene (Gerentaş, Kaypaktepe and Acıdere Formations), Late Miocene-Late Pliocene (Göbekli, Yenipazar and Erendalı Formations) and Plio-Quaternary sedimentary rocks (Asartepe Formation). The Miocene and Plio-Quaternary assemblages are represented by similar depocenters, including lacustrine, fluvial and alluvial-fan environments in the Alaşehir Graben. They are separated by the Late Miocene to Late Pliocene, which represents the depocenter of the floodplain. The floodplain deposits are a monotonous sequence that repeats itself and is not tectonically mobile after the first 140 meters from the stratigraphic bottom based on sub-rounded to rounded clasts from the cataclastic rocks belonging to the ADF. They represent a time of tectonic quiescence during the Late Miocene-Late Pliocene, indicating that tectonic activity on the ADF terminated in the Late Miocene. However, tectonic activity may have rejuvenated in the Plio-Quaternary as indicated by E-W oriented normal faults cutting through the Alaşehir Graben.

Keywords: Alaşehir Detachment Fault, Alaşehir Graben, floodplain deposits, Neogene sequence, sphericity of clasts.

Öz: *Alaşehir Grabeni'nin güney kenarı, aynı gerilmeli rejim içinde sünek-kırılgan kataklastik kayaçlar içeren Alaşehir Sıyrılma Fayı (ASF)ile sınırlanmıştır. Bu sıyrılma fayı, Turgutlu'dan Alaşehir'e kadar yaklaşık 150 km boyunca yüzeylenmiş ve kuzeye düşük bir açıyla (10^0-30^0) eğimli olan yüzeydir. ASF' nin tektonik aktivitesinin sonlanmasını yorumlayan iki ana görüş vardır. Birincisi, fayın son hareketinin, Pliyo-Kuvaterner yüksek açılı normal faylar tarafından kesilmiş olması gerçeğine dayanarak Geç Miyosen'de sona erdiğidir. Diğer görüş ise, ASF' ye ait kataklastik kayaçlarından elde edilen yüzeylenme yaşlarına dayanarak tektonik aktivitesinin Pliyo-Kuvaterner'e kadar devam ettiğidir. Bu tartışmaya katkıda bulunmak için Salihli ve Alaşehir bölgelerindeki ASF'nin*

* Correspondence / *Yazışma*: senfatih81@gmail.com

tavan bloğundaki Neojen istifinin ölçülmüş stratigrafik kayıtlarını bildiriyoruz. Alaşehir Grabeni'nin çökelme evrimi, Miyosen (Gerentaş, Kaypaktepe ve Acıdere Formasyonları), Üst Miyosen-Üst Pliyosen (Göbekli, Yenipazar ve Erendalı Formasyonları) ve Pliyo-Kuvaterner yaşlı tortul kayaçlar (Asartepe Formasyonu) olmak üzere üç pakette tanımlanabilir. Alaşehir Grabeni'nde Miyosen ve Pliyo-Kuvaterner paketleri göl, akarsu ve alüvyal yelpaze ortamları da dahil olmak üzere benzer sedimantasyon ortamları ile temsil edilmektedir. Bu iki dönem taşkın yatağı sedimantasyon ortamını temsil eden Geç Miyosen-Geç Pliyosen zamanıyla ayrılmıştır. Taşkın yatağı tortulları, ASF' ye ait kataklastik kayaçların yarı-yuvarlak-yuvarlak kırıntılarına dayanarak, stratigrafik tabandan itibaren ilk 140 metreden sonra tektonik olarak hareketli olmayan ve kendini tekrarlayan monoton bir dizidir. Bunlar, Geç Miyosen-Geç Pliyosen döneminde oluşan tektonik durgunluk dönemini temsil etmektedir ve ASF'deki tektonik aktivitenin Geç Miyosen döneminde sonlandığını gösterir. Ancak, Alaşehir Grabeni'ni kesen D-B yönlü normal fayların gösterdiği gibi, tektonik aktivite Plio-Kuvaterner'de yeniden canlanmış olabilir.

Anahtar Kelimeler: *Alaşehir Sıyrılma Fayı, Alaşehir Grabeni, Neojen istifi, kırıntıların küreselliği, taşkın yatağı tortuları.*

INTRODUCTION

Continental extensional basins have long attracted the interest of geologists seeking to understand how they form, both depositionally and tectonically (e.g., Yılmaz, 2017; Yang et al., 2021). They characteristically provide the best depositional conditions and consequently contain some of the longest records of continental deposition (e.g., Wright et al., 1999; Gerard, 2003). These records of continental deposition are the product of a complex interplay of several factors, including the rates of extension and subsidence, tectonic activity, volcanism, magmatism, climate and its temporal variability, hydrology, biology and time (e.g., Çemen et al., 1999; Renaut and Ashley, 2002; Yuretich and Ervin, 2002; Mack et al., 2002). One of the markers of tectonic control is sphericity, including angular clasts in the form of pebbles or blocks in depositional settings (e.g., Wright et al., 1999; Gerard, 2003).

An example of sedimentation in such an extensional environment is found in the deposits of the Alaşehir Graben in Western Turkey. There is continuous debate about recent movement of the Alaşehir Detachment Fault (ADF), which is exposed for ~150 km from Turgutlu to Alaşehir and dips to the north at a low-angle (10°-30°) (Figure 1). The recent fault slip activity on the ADF dates to the Late Miocene, based on friction ages obtained from cataclastic rocks (c. 6-5.5 Ma; Ar-Ar muscovite age, Lips et al., 2001). This case is supported by field relationships. The ADF is cut by Plio-Quaternary high-angle normal faults (Şen et al., 2024). There is also a suggestion in the literature that the ADF was active until Plio-Quaternary time (e.g., Seyitoğlu et al., 2002, 2014; Çemen et al., 2006; Seyitoğlu and Işık, 2015). This interpretation is supported by exhumation ages obtained from cataclastic rocks on the detachment fault, which indicate Plio-Quaternary activity (c. 3.10-1.75 Ma, apatite fission track, Gessner et al., 2001; c. 4.5 Ma, Th-Pb monazite, Catlos and Çemen, 2005; c. 3.50-0.80 Ma, apatite fission track and c. 3.5-2.0 Ma, zircon fission track, Buscher et al., 2013; 4 Ma, K-Ar whole rock, Hetzel et al., 2013). The Plio-Quaternary thermal ages indicate that the footwall and hanging wall of the Alaşehir detachment fault were exhumed under the control of Plio-Quaternary high-angle normal faults (Seyitoğlu et al., 2002; Çemen et al., 2006; Şen et al., 2024). However, the margin of error for the Pliocene ages is quite high (c. 4.5 ± 1 Ma; Th-Pb monazite, Catlos and Çemen, 2005). Furthermore, the Pliocene ages (4 Ma, K-Ar whole rock) obtained by Hetzel et al. (2013) are not supported in the dataset (3.5 Ma, apatite and zircon fission track) of Buscher et al. (2013) (see Seyitoğlu et al. (2014) for a detailed review; Table 1, pages of 485-486). The analytical ages are different.

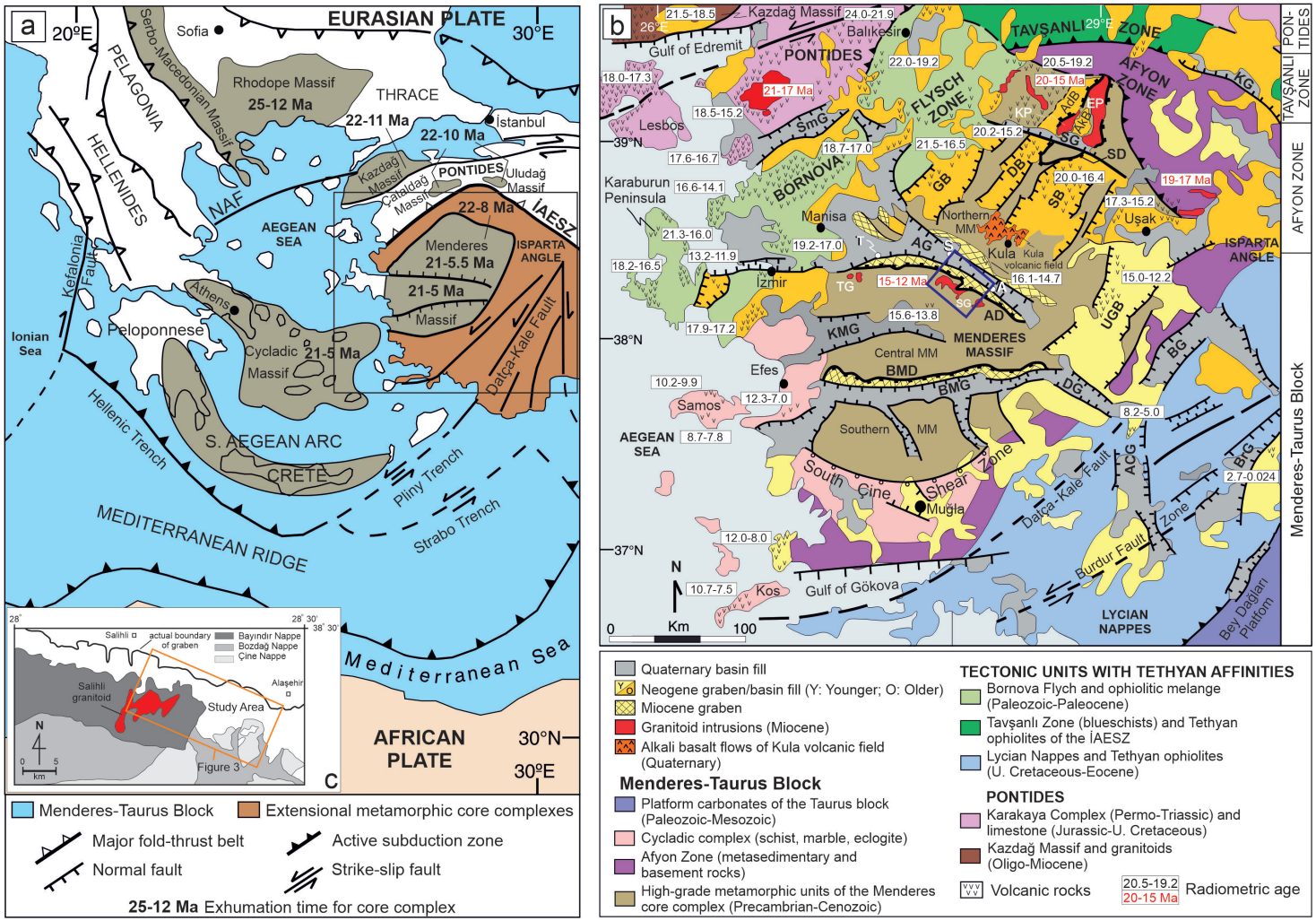

Figure 1. (a) Simplified tectonic map of the Aegean, showing the main plate boundaries and major tectonic structures (modified from Öner and Dilek, 2013). Dark gray areas display the location of metamorphic core complexes in the AEP. The black box represents Figure 1b. Isotopic ages of exhumation are from Lips et al. (2001), Thomson and Ring (2006), Okay et al. (2008), Cavazza et al. (2009), Catlos et al. (2010), Kounov et al. (2015), Wölfler et al. (2017), Heineke et al. (2019), Altunkaynak et al. (2021), and Lamont et al. (2023). **(b)** Simplified geological map of Western Anatolia, displaying the Neogene-Quaternary extensional basins in the Menderes Massif and the surrounding major crustal blocks (after Öner and Dilek, 2013) and **(c)** the

Bayındır-Bozdağ-Çine Nappes of the central submassif belonging to the Menderes Massif in the study area (Konak, 2002). Isotopic ages are from Paton (1992), Platevoet et al. (2008), Helvacı et al. (2009), Ersoy et al. (2014) and Elitez et al. (2018). The area studied is shown in the blue box. A: Alaşehir; AD: Alaşehir Detachment; AG: Alaşehir Graben; ACG: Acıpayam Graben; BG: Baklan Graben; BMD: Büyük Menderes Detachment; BMG: Büyük Menderes Graben; BrG: Burdur Graben; DB: Demirci Basin; DG: Denizli Graben; EP: Eğrizgöz pluton; GB: Gördes Basin; KG: Kütayha Graben; KMG: Küçük Menderes Graben; S: Salihli; SB: Selendi Basin; SD: Simav Detachment; SG: Simav Graben; SG: Salihli granite; SmD: Soma Graben; TG: Turgutlu granitoid; USB: Uşak-Güre Basin.

Şekil 1. (a) *Ege bölgesinin ana levha sınırlarını ve başlıca tektonik yapıları gösteren basitleştirilmiş tektonik haritası (Öner ve Dilek, 2013'ten değiştirilmiştir). Koyu gri alanlar AEP' deki metamorfik çekirdek komplekslerinin yerini göstermektedir. Siyah kutu Şekil 1b'yi göstermektedir. Kazı zamanına ait izotopik yaşlar Lips vd. (2001), Thomson ve Ring (2006), Okay vd. (2008), Cavazza vd. (2009), Catlos vd. (2010), Kounov vd. (2015), Wölfler vd. (2017), Heineke vd. (2019), Altunkaynak vd. (2021), Lamont vd. (2023)'den alınmıştır.* ***(b)*** *Batı Anadolu'nun basitleştirilmiş jeoloji haritası, Menderes Masifi'ndeki ve çevresindeki büyük kabuk bloklarındaki Neojen-Kuvaterner ekstansiyonel havzalarını (Öner ve Dilek, 2013'e göre) ve* ***(c)*** *çalışma alanında Menderes Masifi'ne ait merkezi alt masifin Bayındır-Bozdağ-Çine Napları' nı (Konak, 2002) göstermektedir. İzotopik yaşlar Paton (1992), Platevoet vd. (2008), Helvacı vd. (2009), Ersoy vd. (2014) ve Elitez vd. (2018) tarafından alınmıştır. Bu çalışmada çalışılan alan mavi kutuda gösterilmiştir. A: Alaşehir; AD: Alaşehir Sıyrılma Fayı; AG: Alaşehir Grabeni; ACG: Acıpayam Grabeni; BG: Baklan Grabeni; BMD: Büyük Menderes Sıyrılma Fayı; BMG: Büyük Menderes Grabeni; BrG: Burdur Grabeni; DB: Demirci Havzası; DG: Denizli Grabeni; EP: Eğrizgöz plütonu; Gördes Havzası; KG: Kütayha Grabeni; KMG: Küçük Menderes Grabeni; S: Salihli; SB: Selendi Havzası; SD: Simav Sıyrılma Fayı; SG: Simav Grabeni; SG: Salihli graniti; SmD: Soma Grabeni; TG: Turgutlu granitoyidi; USB: Uşak-Güre Havzası.*

The Late Miocene-Pliocene in the Alaşehir Graben is a highly critical time interval based on these discussions. Although some researchers (e.g. Seyitoğlu et al., 2002; Purvis and Robertson, 2005; Çiftçi and Bozkurt, 2009) have examined measured stratigraphic logs in the fills of the Alaşehir Graben, we believe that no light could be shed on this discussion because they could not provide data about fault slip activity and Late Miocene-Pliocene time. Therefore, measured stratigraphic logs for the Miocene-Pliocene sedimentary rocks by Şen (2004) and Ağırbaş (2006) are used to reconstruct recent movement of the ADF from a new perspective in this paper.

Geology of Western Anatolia

Western Anatolia is located in an extensional region, known as the Aegean Extensional Province (AEP) active from the Neogene to the Plio-Quaternary, in the convergent setting of African-European collision (Bozkurt, 2001; Çemen et al., 2006; Jolivet and Brun, 2010; van Hinsbergen et al., 2010) (Figure 1a). This tectonic setting has led to the formation of core complexes during ongoing subduction-related slab-edge processes[1] along the Hellenic-Cyprian trenches (e.g. van Hinsbergen et al., 2010; Biryol et al, 2011). This led to the exhumation of metamorphic core complexes, including the Rhodope, Kazdağ, Uludağ, Menderes and Cycladic core complexes from north to south, during the Oligo-Miocene (Wawrzenitz and Krohe, 1998; Okay and Satır, 2000; Işık et al., 2003; Okay et al., 2008; Catlos et al., 2010; Kounov et al., 2015; Wölfler et

1 Subduction transform edge propagator (STEP, also known as tear) faults occur at slab edges (Govers and Wortel, 2005). STEP faults produce tears in the slab and generally propagate perpendicular to the subduction strike (Nijholt and Govers, 2015). Most of them show vertical motion between the two blocks of the underthrusting plate on either side of the STEP fault and normal to the strike-slip motion in the upper plate (Baes et al., 2011; Govers and Wortel, 2005). In Western Anatolia, the slab edge processes are related to the northward subduction of the African slab below Eurasia (Le Pichon and Angelier, 1979; Meulenkamp et al., 1988; van Hinsbergen et al., 2005, 2010; Edwards and Grasemann, 2009; Biryol et al., 2011; Soder et al., 2016).

al., 2017; Heineke et al., 2019; Lamont et al., 2023) (Figure 1a). Tomographic studies indicate that slab-edge processes and associated back-arc extension are the dominant factors in the extensional tectonics of the Aegean region (van Hinsbergen et al., 2005, 2010; Faccenna et al., 2003, 2006, 2013; Çemen et al., 2006; Gans et al., 2009; Biryol et al., 2011; Philippon et al., 2012; Jolivet et al., 2013; Menant et al., 2016). The extensional domain in the Aegean region acts through large-scale extensional detachment faults and high-angle normal faults along which core complexes are exhumed, and each core complex accommodates a different amount of extension and rotation depending on the back-arc scenario (McKenzie, 1978; Le Pichon and Angelier, 1979, 1981; Mercier, 1981; Jackson and McKenzie, 1988; Meulenkamp et al., 1988, 1994; Kiseel and Laj, 1988; Jolivet and Patriat, 1999; Jolivet and Faccenna, 2000; Okay and Satır, 2000; Philippon et al., 2012; Gessner, et al., 2013; Jolivet et al., 2013; Uzel et al., 2015) (Figure 1a, b).

The Menderes-Taurus Block and the Pontides collided before the Oligo-Miocene (van Hinsbergen et al., 2010; Öner and Dilek, 2013; Uzel et al., 2015) (Figure 1a). The Rhodope and Kazdağ-Uludağ core complexes in the Western Pontides and the Menderes and Cycladic core complexes in the West Menderes-Taurus Block moved together in the same geodynamic setting during the Oligo-Miocene. The Menderes-Taurus Block was added to the Pontides during the Middle Ypresian (c. 53-50 Ma; Akbayram et al., 2016) after the Kırşehir Block collided with the Pontides during the Paleocene-Eocene transition (c. 56 Ma; Hippolyte et al., 2010; Espurt et al., 2014). The collision associated with the destruction of the Tethys Ocean, which was located between the Menderes-Taurus Block and the Pontides, lasted ~25 million years (Şen, 2020), and the final time of the collision is represented by the late Oligocene (c. 27 Ma; Elmas et al., 2016). Thus, after docking of the two continental blocks, Western Anatolia began to extend during the Oligo-Miocene as a result of roll-back of the African oceanic lithosphere, which is subducted beneath Eurasia along the Cyprian and Aegean arcs (van Hinsbergen et al., 2010; Biryol et al, 2011). The metamorphic core complexes developed during the Oligo-Miocene to the Late Miocene under the control of detachment faults, and high-grade metamorphic rocks began to be exhumed north of the Cyprian and Aegean trenches (e.g., Okay and Satır, 2000; Lamont et al., 2023). Western Anatolia experienced westward escape at about 6-5 Ma as a result of the North Anatolian Fault Zone, which was preceded by a major displacement zone known as the North Proto-Anatolian Transform. This transform fault began in the mid-to-late Miocene and connected to the Bitlis Suture in eastern Anatolia (Dewey and Şengör, 1979; Şengör et al., 2005). This indicates that the interaction between back-arc extension and westward displacement of Anatolia is roughly related to the post-Late Miocene tectonic history of Western Anatolia, following only back-arc extension driven by slab rollback in Oligo-Miocene to Late Miocene time. After the Late Miocene, extension was controlled by Plio-Quaternary high-angle faults (e.g., Bozkurt and Sözbilir, 2004; Şen et al., 2024), resulting in a two-stage extensional phase consisting of Miocene and Plio-Quaternary extensional phases in Western Anatolia.

Grabens in Western Anatolia

It is generally agreed that extension in Western Anatolia was initiated by the latest Oligocene-Early Miocene and formed in two distinct extensional phases; (a) latest Oligocene-Miocene metamorphic core complex formation in the footwall of what are now low-angle normal faults; and (b) post-Miocene modern graben formation as a result of Plio-Quaternary high-angle normal faults (Bozkurt and Park, 1994; Hetzel et al., 1995; Lips et al., 2001; Yılmaz et al., 2000; Gessner et al 2001, 2013; Ring et al., 2003; Bozkurt, 2003;

Bozkurt and Sözbilir, 2004; Çemen et al., 2006; Thomson and Ring, 2006; Özsayın and Dirik, 2007; Çiftçi and Bozkurt, 2008, 2009, 2010; Şen et al., 2024). These extensional phases evolved in two possible ways (i) continuously without temporal interruption from Oligo-Miocene to recent times (e.g. Seyitoğlu et al., 2000, 2002, 2004; Çemen et al., 2006; Glodny and Hetzel, 2007; Seyitoğlu and Işık, 2015) or (ii) episodically with multiple phases of extension separated by contraction periods during the Late Miocene to Pliocene (Koçyiğit et al., 1999; Bozkurt and Sözbilir, 2004; Bozkurt and Rojay, 2005; Rojay et al., 2005; Emre and Sözbilir, 2007). Şen et al. (2024) recently showed that the Late Miocene-Late Pliocene was a tectonically quiescent period between two rifting periods in the Miocene and the Plio-Quaternary.

Western Anatolia consists of (a) NNE-SSW-trending grabens filled with Lower Miocene and younger deposits of siliciclastic, volcanoclastic, and volcanic rocks, and (b) E-W-trending grabens filled with Lower Miocene and younger siliciclastic rocks (Bozkurt, 2001; Öner and Dilek, 2013; Seyitoğlu and Işık, 2015) (Figure 1b). The NNE-SSW-trending grabens include the Gördes, Demirci, Uşak-Güre, Selendi and Baklan grabens, which are bounded by high-angle normal faults with strike-slip components (Yılmaz et al., 2000; Bozkurt, 2001) (Figure 1b). The E-W-trending basins are the Simav, Alaşehir, Küçük Menderes, and Büyük Menderes grabens, which are bounded by high-angle to moderately dipping normal faults that are seismically active (Yılmaz et al., 2000; Bozkurt, 2001) (Figure 1b). In the footwalls of the E-W trending grabens, the NNE-SSW trending grabens form 'hanging grabens' (Yılmaz et al., 2000; Seyitoğlu and Işık, 2015). The seismic profiles by Gürer et al. (2001) distinguish trapped structures and sedimentary rocks of the NNE-SSW trending grabens.

Geology of the Alaşehir Graben

Structural framework

Faults are the main structural elements in the Alaşehir Graben. These are divided into three groups (Şen et al., 2024). (a) The E-W trending, N-dipping (0° to 30°), currently low angle normal/detachment fault, called the ADF is extensively exposed along the southern margin of the Alaşehir Graben (e.g. Emre, 1996; Koçyiğit et al., 1999; Işık et al., 2003; Şen et al., 2024) (Figures 1b, 2a, b, c and 3). The ADF forms a cataclastic zone of 60 to 150 m thickness as the deep part of the fault approaches the surface (e.g. Işık et al., 2003). (b) Low-angle (5°-30°) normal faults, which have no cataclastic rocks, with E-W strike and N- and S-dips. They are synthetic and antithetic faults of the ADF and join to it (Şen, 2004; Ağırbaş, 2006; Şen et al., 2024) (Figure 3). The initial position of these two types of faults was high-angle (Seyitoğlu et al., 2004; Çemen et al., 2005, 2006) and the original position had a dip of 55°-75° during the Miocene (Şen et al., 2024). (c) E-W-trending, N-dipping (≥ 40°) actual graben-bounding normal faults have variable sizes with a graben-facing step-like pattern dominated by first-order major and second-order synthetic to antithetic faults (Bozkurt and Sözbilir, 2004; Çiftçi and Bozkurt, 2009; Şen et al., 2024). The Plio-Quaternary high-angle normal faults control the southern margin of the Alaşehir Graben as well as the deformation pattern within the graben fill (Emre, 1996; Koçyiğit et al., 1999; Bozkurt and Sözbilir, 2004; Çiftçi and Bozkurt, 2009). The alluvial fans and alluvium of the Alaşehir Graben are cut by modern graben-bounding normal major faults, which caused the Alaşehir earthquake of 28 March 1969 (M=6.9) forming a N50°-85°W-trending surface rupture of 30-35 km in length (Arpat and Bingöl, 1969; Eyidoğan and Jackson, 1985) (Figures 3 and 4). The Plio-Quaternary high-angle normal faults cross-cut and displace the ADF and its synthetic and antithetic faults (Şen, 2004, 2016; Ağırbaş, 2006; Şen and Ağırbaş, 2012; Ağırbaş and Şen, 2012; Şen et al., 2024) (Figures 3 and 4).

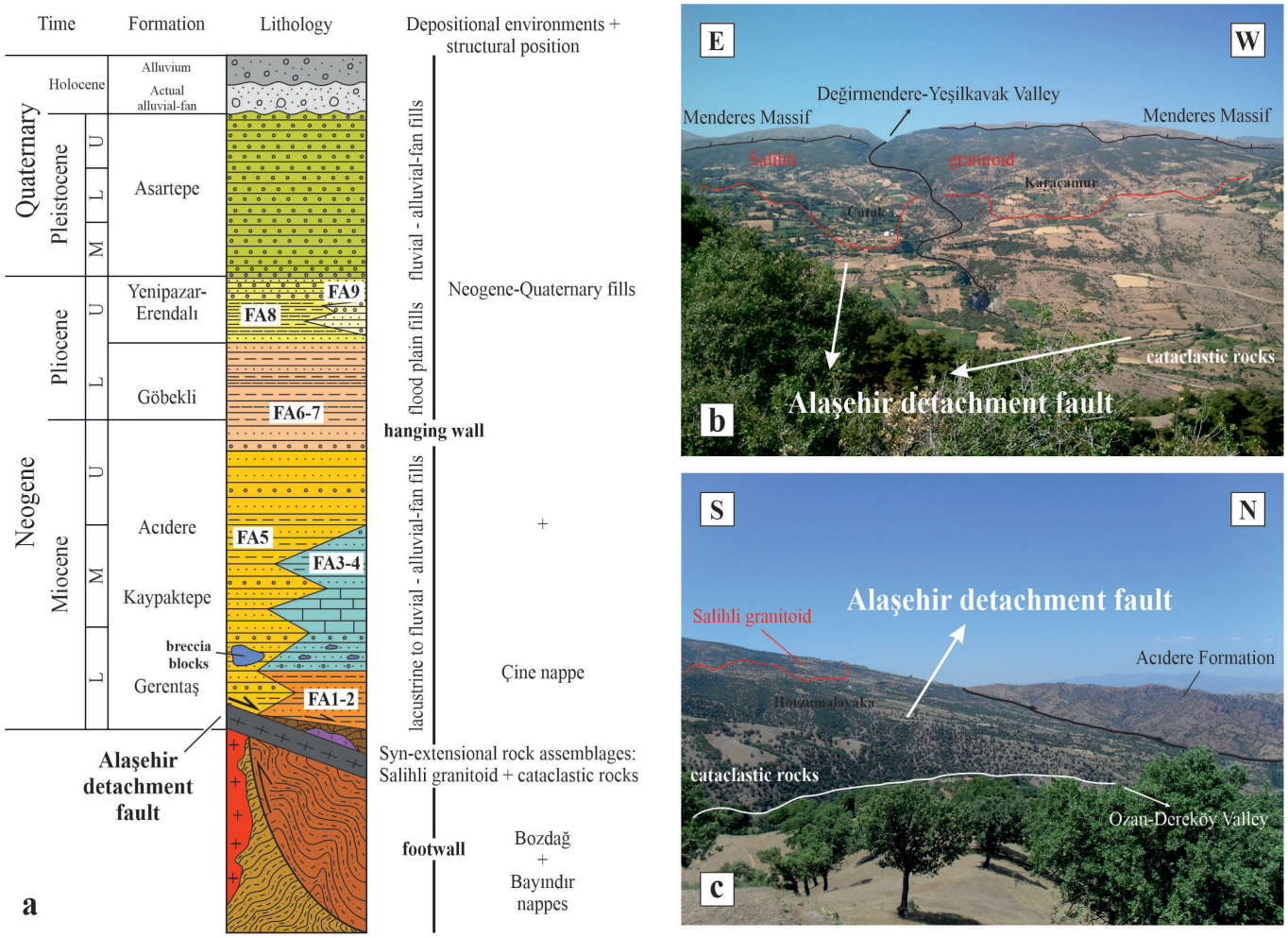

Figure 2. **(a)** Stratigraphic column section for the southern margin of the Alaşehir Graben in the Salihli and Alaşehir areas (taken from Şen et al., 2024), **(b-c)** Photographs showing the Alaşehir Detachment Fault in Alaşehir Graben (taken from Şen, 2004 and Ağırbaş, 2006). Description of facies associations and constituent facies are given in Tables 1–7.

Şekil 2. ***(a)*** *Salihli ve Alaşehir bölgelerinde Alaşehir Grabeni'nin güney kenarının stratigrafik kolon kesiti (Şen vd., 2024'ten alınmıştır),* ***(b-c)*** *Alaşehir Grabeni'ndeki Alaşehir Sıyrılma Fayı'nı gösteren fotoğraflar (Şen, 2004 ve Ağırbaş, 2006'dan alınmıştır). Fasiyes birliktelikleri ve bileşen fasiyeslerin tanımı Tablo 1-7'de verilmiştir.*

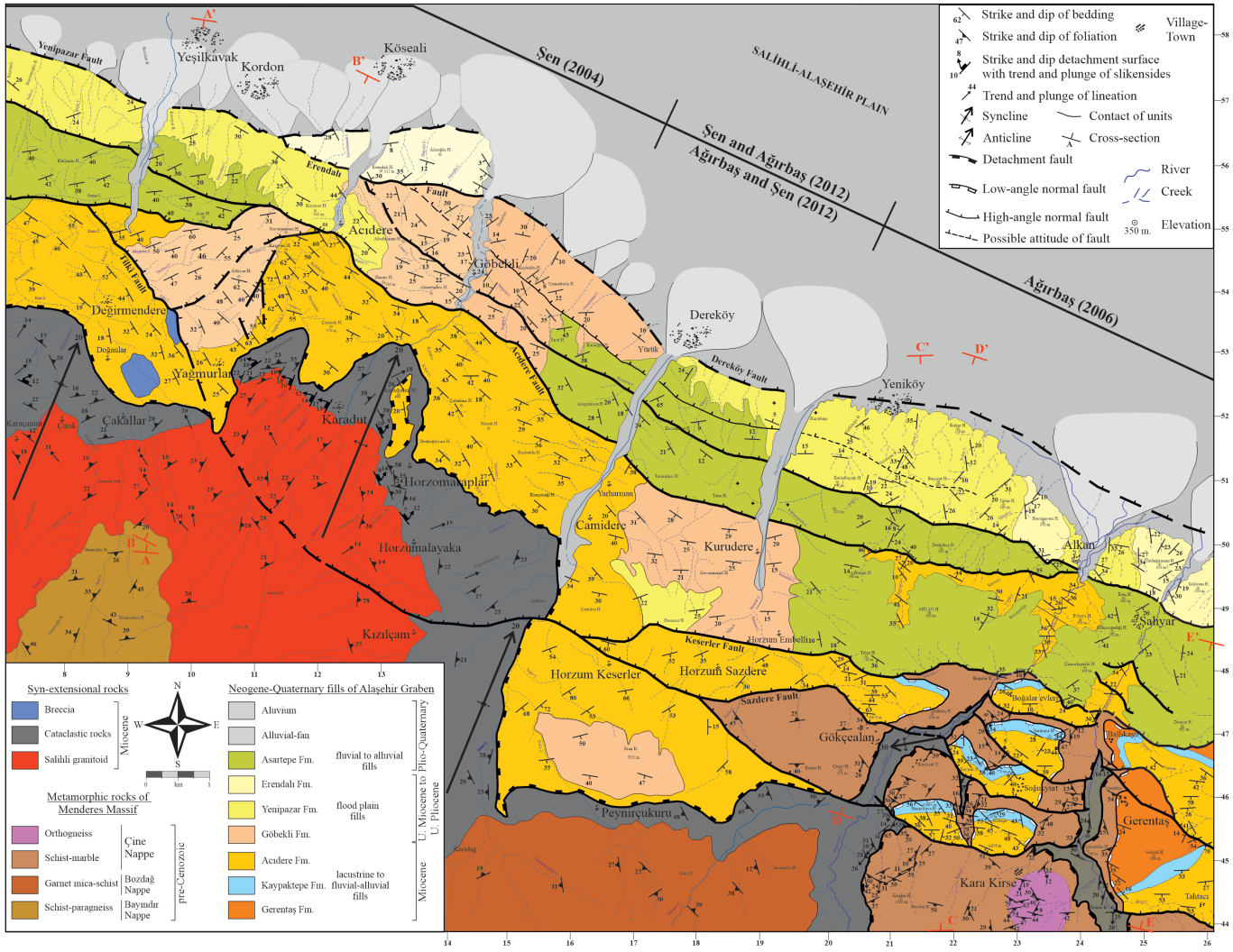

Figure 3. Geological map of the southern margin of the Alaşehir Graben in the area between Karaçamur in the Salihli and Tahtacı in Alaşehir (taken from Şen, 2004; Ağırbaş, 2006; Şen and Ağırbaş, 2012; Ağırbaş and Şen, 2012; Şen et al., 2024).

Şekil 3. *Salihli'deki Karaçamur ile Alaşehir'deki Tahtacı arasındaki Alaşehir Grabeni'nin güney kenarının jeolojik haritası (Şen, 2004; Ağırbaş, 2006; Şen ve Ağırbaş, 2012; Ağırbaş ve Şen, 2012 ve Şen vd., 2024'ten alınmıştır).*

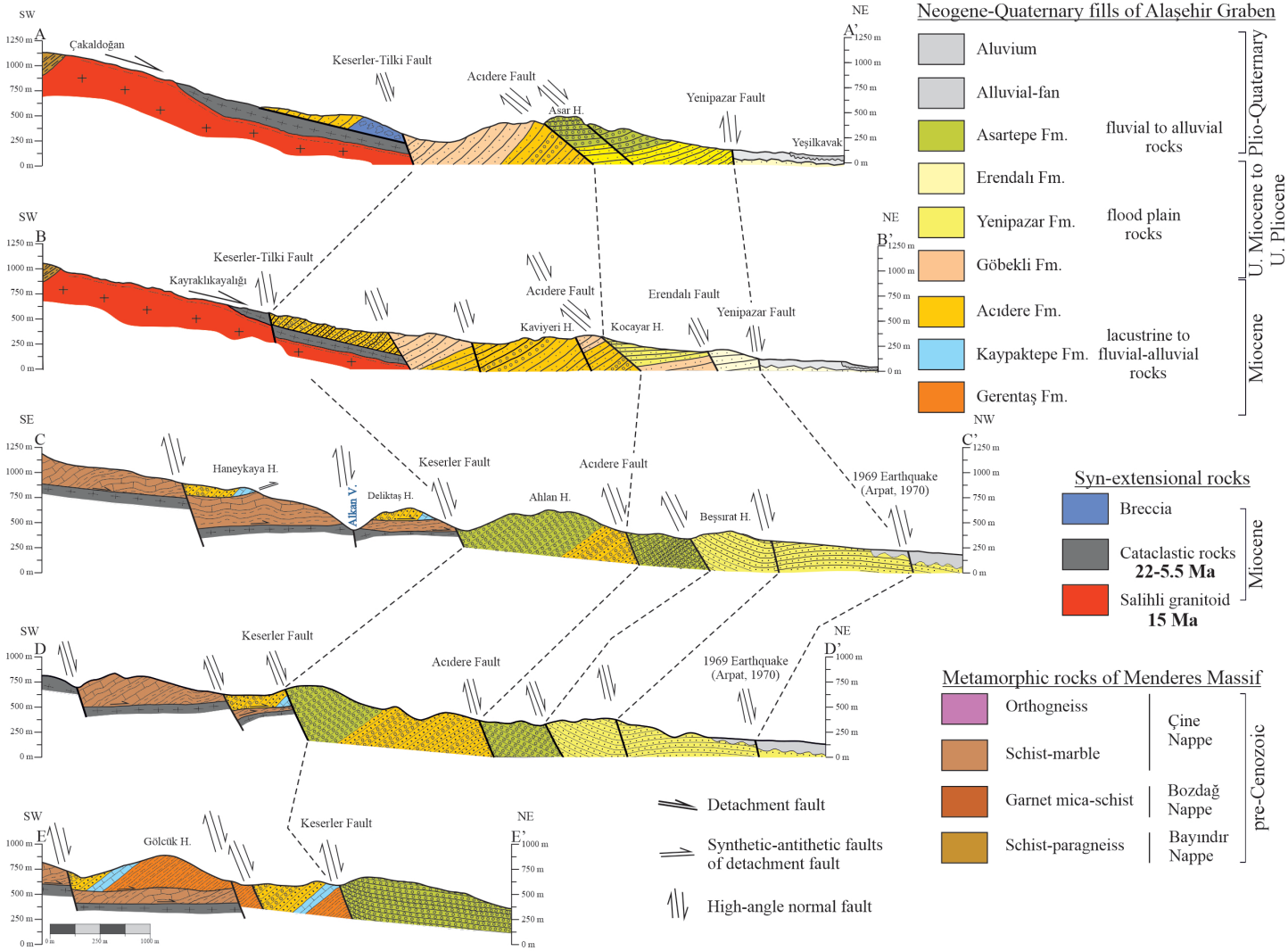

Figure 4. Geological cross-sections for the southern margin of the Alaşehir Graben. The locations of cross-sections in the study area are shown in Figure 3 (taken from Şen, 2004 for A-A' and B-B; Ağırbaş, 2006 for C-C', D-D' and E-E).

Şekil 4. *Alaşehir Grabeni' nin güney kenarındaki jeolojik enine kesitler. Çalışma alanındaki kesitlerin yerleri Şekil 3'te gösterilmiştir (A-A' ve B-B için Şen, 2004'ten; C-C', D-D' ve E-E için Ağırbaş, 2006'dan alınmıştır).*

There are two main groups of folds on the southern margin of the Alaşehir Graben. (a) Narrow N-S broad anticlines and synclines, which are north-vergent, plunging, asymmetric to overturned geometry, are often observed in association with south-dipping small-scale thrust and reverse faults in the Miocene fills (Çiftçi and Bozkurt, 2008). They have NE-trend and plunge mainly NE, with E–W-trend plunging mainly west in the Salihli and Alaşehir segments in the footwall and hanging wall of the ADF (Şen, 2004; Ağırbaş, 2006; Şen et al., 2024) (Figure 3). They are related to extensional structures formed by layer-parallel shortening during the Miocene (Şengör and Bozkurt, 2012; Şen et al., 2024). (b) Broad E-W trending anticlines and synclines, which have fold axes sub-parallel to the graben bounding faults, are commonly observed in the Miocene fills (Seyitoğlu, 1999; Koçyiğit et al., 1999; Seyitoğlu et al., 2000; Bozkurt and Sözbilir, 2004; Çemen et al., 2006). They are due to the movement of Miocene fills over listric normal faults, forming drag folds and roll-over anticlines during ongoing extension, and displacement on Plio-Quaternary high-angle normal faults is responsible for their formation (Seyitoğlu et al., 2000, 2004; Çemen et al., 2006; Seyitoğlu and Işık, 2015).

Tectono-stratigraphic framework

The Alaşehir Graben is located on the boundary between the northern and central sectors of the Menderes Massif (Bozkurt, 2000, 2001; Öner and Dilek, 2013; Seyitoğlu and Işık, 2015) (Figure 1b). The study area is the Central sub-massif of the Menderes Massif, which forms the southern edge of the Alaşehir Graben between Salihli and Alaşehir (Figure 1b-c). The Central sub-massif of the Menderes Massif in the study area contains a nappe suite, including the Bayındır, Bozdağ and Çine Nappes, which formed during the Late Ediacaran to Early Cambrian and Early Cenozoic (Ring et al., 1999; Dora et al., 2001; Gessner et al., 2001) (Figure 1b). The emplacement of the nappes occurred during the Early Eocene as a result of closure of the Tethys Ocean along the İzmir-Ankara-Erzincan suture (e.g., Okay and Tüysüz, 1999; Gessner, 2000; Gessner et al., 2001). The Bayındır Nappe is structurally the lowest nappe unit and contains mica-schist and paragneiss with greenschist-amphibolite metamorphism conditions (Dora et al., 2001; Erdoğan and Güngör, 2004). The Bozdağ Nappe consists of amphibolite facies garnet-mica schists (Gessner et al., 2001). The Çine Nappe is structurally the uppermost nappe unit and contains orthogneisses cutting schists and marbles alternating with metabasite with amphibolite to granulite metamorphic conditions (Oberhänsli et al. 1997; Candan et al. 2001).

The tectonostratigraphy of the study area is structurally separated by the ADF (Figures 2, 3 and 4). The footwall of the ADF consists of the Bayındır and Bozdağ Nappes and the syn-extensional Salihli granitoid (c. 15 Ma; Glodny and Hetzel, 2007) intruding the Bayındır Nappe (Figures 2, 3 and 4). The hanging wall of the ADF contains the Çine Nappe and Neogene-Quaternary sedimentary rocks. Miocene deposits tectonically overlie the Çine Nappe along the ADF (Şen et al., 2024) (Figures 2, 3 and 4).

The Neogene-Quaternary sedimentary rocks with thickness of c. 3000 m (Çiftçi and Bozkurt, 2009) include Miocene (Gerentaş, Kaypaktepe and Acıdere Formations), Upper Miocene-Upper Pliocene (Göbekli, Yenipazar and Erendalı Formations) and Plio-Quaternary deposits (Asartepe Formation) (Figure 2). Although the nomenclature and contents of the Neogene-Quaternary sedimentary rocks in the Alaşehir Graben have been interpreted by different researchers (e.g. Emre, 1996; Koçyiğit et al., 1999; Seyitoğlu et al., 2002; Çiftçi and Bozkurt, 2009), the generalized stratigraphic section is given based on the stratigraphic dataset of Şen et al. (2024) and Şen (2004) and Ağırbaş (2006) because other researchers do not reflect the nature of the Alaşehir Graben in their columnar sections (Figure 2) (see Şen et al., 2024 for a detailed review).

The Alaşehir Graben succession forms a transgressive series beginning with Miocene

lacustrine shales, mudstones, limestones, sandstones and fluviatile sandstones, and conglomerates, overlain by Upper Miocene-Upper Pliocene floodplain mudstones sandstones and conglomerates. The floodplain deposits grade into a clastic sequence of semi-lithified sandstone and conglomerate (Şen et al., 2024). The Miocene fills are divided into three units of the Gerentaş, Kaypaktepe and Acıdere Formations (Figures 2, 3 and 4). In the Alaşehir area, the Gerentaş Formation contains shale and mudstone alternating with conglomerate-sandstone conformably overlain by mudstone and conglomerate with limestone interbeds of the Kaypaktepe Formation (Ağırbaş, 2006; Şen et al., 2024). They were deposited in a lacustrine environment during the Early to Middle Miocene (Ediger et al., 1996; Seyitoğlu et al., 2002; Şen and Seyitoğlu, 2009), and tectonically overlie the Çine Nappe, which is structurally located above the Alaşehir segment of the ADF (Şen et al., 2024) (Figures 2, 3 and 4). They pass laterally and vertically into the Acıdere Formation, which consists of mudstone and sandstone (Ağırbaş, 2006; Şen et al., 2024). In the Salihli area, the Acıdere Formation contains mudstone and sandstone alternating with conglomerate (Emre, 1996). It was deposited in a fluvial and alluvial depocenter (Emre, 1996) during the Early to Late Miocene that tectonically overlies the Bayındır and Bozdağ Nappes, which structurally overlie the Salihli segment of the ADF (Şen, 2004; Şen et al., 2024) (Figure 2–4). The Upper Miocene-Upper Pliocene floodplain fills are divided into three units of the Göbekli, Yenipazar and Erendalı Formations (Figure 2–4). The Acıdere Formation is conformably overlain by the Upper Miocene-Lower Pliocene Göbekli Formation, which consists of mudstones, sandstones and conglomerates (e.g., Emre, 1996; Purvis and Robertson, 2005). It passes vertically into the Yenipazar Formation, which consists of fine-grained clastics, and laterally into the Erendalı Formation, which consists of fine- and coarse-grained clastics and has Upper Pliocene age (Sarıca, 2000). The Yenipazar Formation passes vertically into the Asartepe Formation, which consists of coarse-grained clastics in the alluvial-fan depocenter (Emre, 1996; Şen, 2004; Ağırbaş, 2006; Şen et al., 2024), and depositional age is Plio-Quaternary (Sarıca, 2000) (Figure 2–4).

MATERIAL and METHODS

Stratigraphic measurements were made within exhumed Miocene-Pliocene sedimentary rocks along the southern margin of the Alaşehir Graben, between the Salihli and Alaşehir areas, based on studies by Şen (2004) and Ağırbaş (2006) (Şen et al., 2024) (Figures 3, 5). Geological mapping was carried out in the summer of 2003 without examining previous studies. The map study was made according to the colors and dominant lithology of the rocks, named as a-unit, b-unit, c-unit, etc. When the field work was completed and the office work started, the formation names were assigned based on previous studies (Şen, 2004; p. 12; Ağırbaş, 2006; p. 12).

The stratigraphic relationships of the rocks were determined by tracing the contacts during geological mapping studies. The measured stratigraphic logs were made with a 150 cm long Jacob's stick divided into centimeters. During the stratigraphic measurements, both the actual thickness of the layers and the characteristics of the units along the section line were recorded in the field. These methods were chosen for high-precision measurements of stratigraphic variations within the Neogene sedimentary sequence of the Alaşehir Graben. Lithological diversity and structural accessibility were considered in the selection of measurement sites. The measured stratigraphic logs were made by Fatih Şen and Hakan Ağırbaş at seven different locations in the Salihli and Alaşehir areas in the summer of 2003. The routes and locations of the measured stratigraphic logs are shown in Figure 5. The results of the stratigraphic measurements are summarized below.

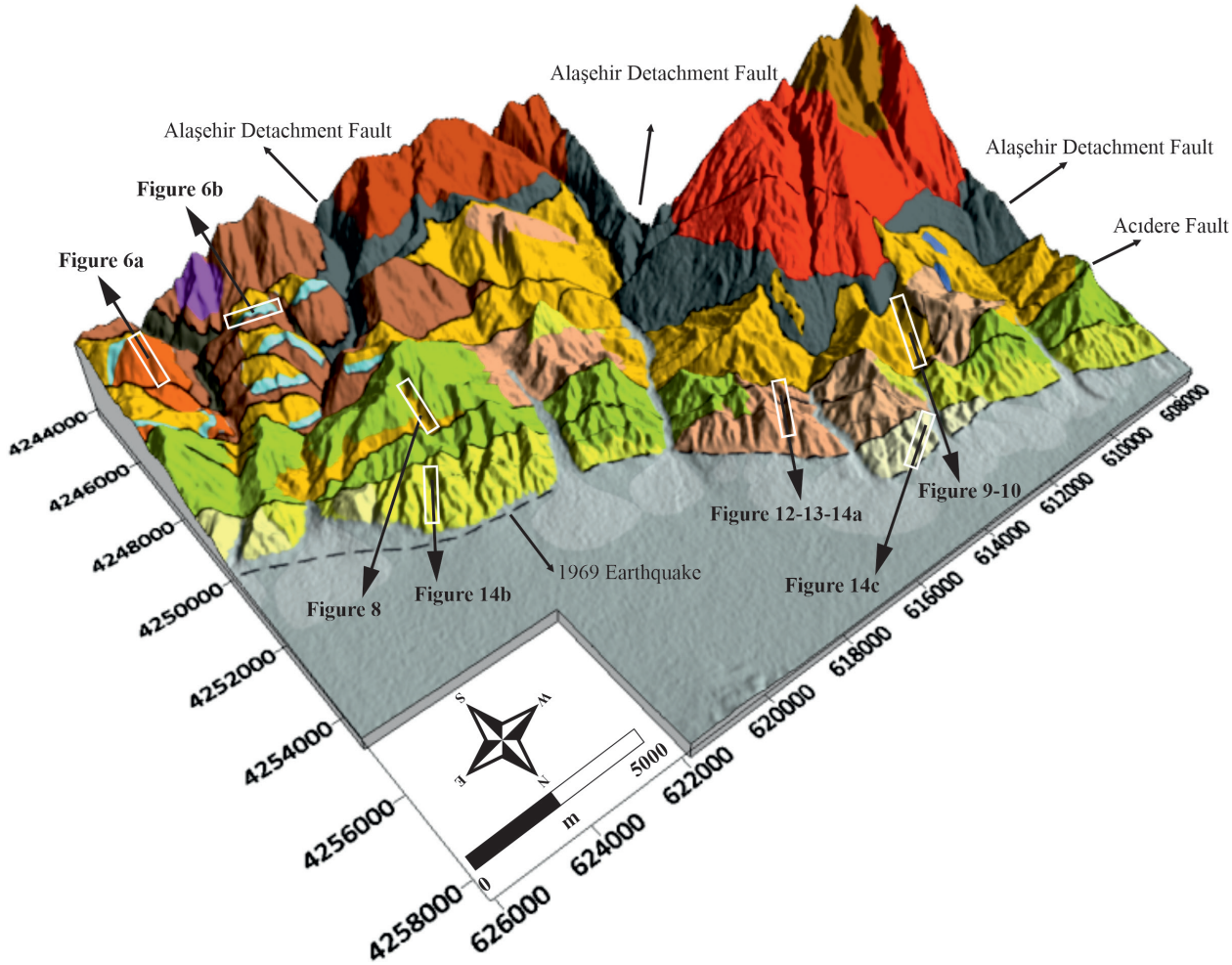

Figure 5. Geological map using 3D imagery for the southern margin of the Alaşehir Graben. Note the routes and locations of the measured stratigraphic logs.

Şekil 5. *Alaşehir Grabeni' nin güney kenarında 3B görüntüleme kullanılarak elde edilen jeolojik harita. Ölçülü stratigrafik kesitlerin rotalarını ve yerlerini fark edin.*

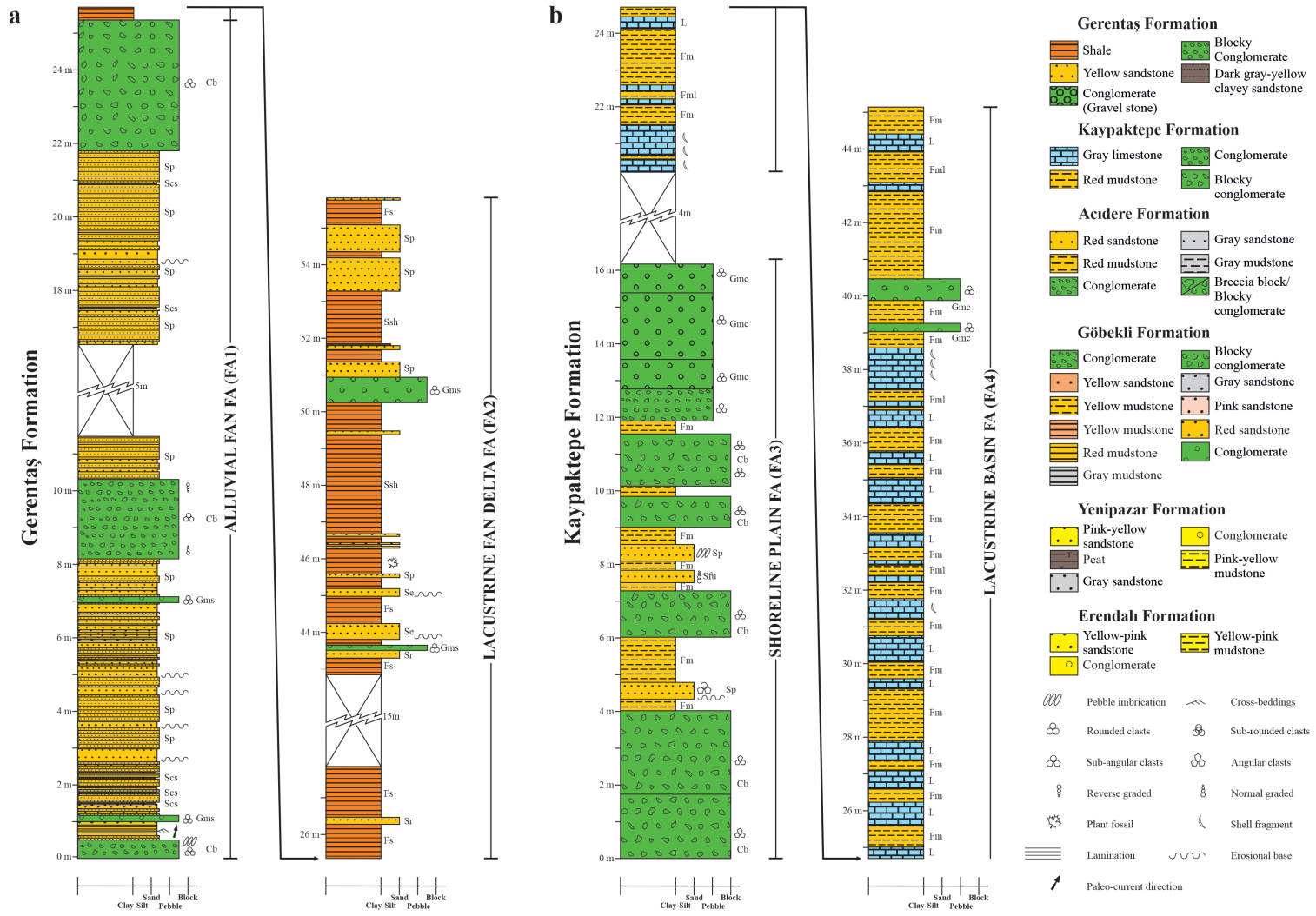

Figure 6. Measured stratigraphic logs of the Gerentaş Formation **(a)** and Kaypaktepe Formation **(b)** in the Alaşehir area (taken from Ağırbaş, 2006). See Figure 5 for location.

Şekil 6. *Alaşehir bölgesindeki Gerentaş Formasyonu (a) ve Kaypaktepe Formasyonu'nun (b) ölçülü stratigrafik kesitleri (Ağırbaş, 2006'dan alınmıştır). Konum için Şekil 5'e bakınız.*

RESULTS

In this section, each Neogene formation on the southern margin of the Alaşehir Graben is interpreted in terms of facies associations. This is based on the facies defined in the measured stratigraphic logs (Figures 6, 8, 9, 10, 11, 12 and 13). The measured thickness of the facies associations in the logs is much less than their actual thickness. This is due to dense forest areas and normal faulting, which makes it impossible to measure a complete section without a gap. The measured stratigraphic logs were therefore only used to characterize the facies of the formations. Precise cross-sections were used to determine the true thickness of the formations (Figure 4)

Gerentaş Formation

The Gerentaş Formation is well-exposed southwest of the Alaşehir area in the village of Gerentaş (Figure 3). The exact thickness of the Gerentaş Formation remains uncertain due to the tectonic overlay of high-grade metamorphic rocks from the Çine Nappe (Figure 3). However, based on E-E' cross-section analysis, its maximum estimated thickness is ~ 600 m (Figure 4), whereas measured stratigraphic logs at Gölçük Hill indicate a thickness of 55 m (Figure 6a) (Ağırbaş, 2006), suggesting significant structural or erosional variation. A total of eight lithofacies were defined by bed type, grain size and primary sedimentary structure (Table 1). This lithofacies diversity is grouped into two main facies associations of FA1 (alluvial fan facies association) and FA2 (lacustrine fan delta facies association) (Table 2). FA1 refers to coarse-grained beds in the lower levels of the Gerentaş Formation and FA2 refers to fine-grained beds in the middle and upper levels of the Gerentaş Formation (Figure 6).

Table 1. Dominant facies, facies descriptions and interpretations for the Gerentaş Formation.
Çizelge 1. *Gerentaş Formasyonu' nun baskın fasiyesleri, fasiyes tanımları ve yorumları.*

Facies	Description	Interpretation
Cb, blocky conglomerates	Blocky conglomerates with sandy to gravelly matrix, matrix-supported, chaotic, poorly sorted to unsorted, polymictic angular and sub-angular clasts, irregular top, locally reverse and normal grading, pebbly imbrications; dimensions: bed thickness up to 3.5 m; lateral extent tens to hundred meters	Debris flow
Gms, matrix-supported gravel stones	Gravelstones with sandy matrix, poorly bedded, poorly sorted, polymictic subangular-rounded clasts, locally fining upward with an erosive base with or without a lag; dimensions: bed thickness up to 1 m; lateral extent few tens of meters	Debris flow to channel (channel fill)
Sp, pebbly sandstones	Coarse-grained sandstones, pebbly, poorly bedded, moderately cemented, erosive base; dimensions: bed thickness up to 50 cm; lateral extent few tens of meters	Deposits of flash floods
Scs, clayey sandstone	Clayey sandstone with argillaceous matrix, laminated; bed thickness up to 5 cm; lateral extent tens of meters	Channel fill-waning currents in channel
e, erosive-based sandstones	Coarse-grained sandstone, moderate to poorly sorted, yellow colored, lenses, cross bedded, erosive base, fining upward; dimensions: bed thickness up to 57 cm; lateral extent up to 5 meters	Scour-fills
Sr, rippled sandstones	Medium- to fine-grained sandstone, laminated at the lower parts of the bed and rippled at the top; dimensions: bed thickness up to 20 cm; lateral extent tens of meters	Subaqueous deposits in lower flow regime
Ssh, alternation of sandstone-shale	Fine-grained sandstone and shale, laminated, moderately cemented; dimensions: bed thickness up to 40 cm; lateral extent tens of meters	Deposition from suspension with episodic turbulent flows - low-energy (lacustrine)
Fs, shales	Shales, wavy laminated, very bituminous, abundant plant remnants, gray colored; dimensions: bed thickness up to 15 cm; lateral extent tens of meters	Deposition from suspension - low-energy (lacustrine)

Table 2. Facies associations of the Neogene succession at the southern margin of the Alaşehir Graben.

Çizelge 2. *Alaşehir Grabeni'nin güney kenarındaki Neojen istifinin fasiyes ilişkileri.*

Facies associations	Constituent lithofacies
FA1, Alluvial-fan facies associations	Cb, Gms, Sp, Scs in Table 1
FA2, Lacustrine fan delta associations	Gms, Sp, Se, Sr, Ssh, Fs in Table 1
FA3, Shoreline plain facies associations	Cb, Gmc, Sp, Sfu, Fm in Table 3
FA4, Lacustrine basin facies associations	Gmc, Fm, Fml, L in Table 3
FA5, Alluvial-fan/fluvial facies associations	Cb, Cbr, Gcg, Sp, Sc, Se, Ssc, Sl, M in Table 4
FA6, Alluvial-fan/fluvial facies associations	Cb, Sp, Ss, Sl, Se, S, M, Csm in Table 5
FA7, Floodplain facies associations	Gms, Sp, Se, Sc, Sl, SS, Ssc, Csm, S, M in Table 5
FA8, Floodplain facies associations	Gms, Sp, Sfg, M, C in Table 6
FA9, Floodplain facies associations	Gms, Sfg, Scg, M in Table 6

FA1: Alluvial-fan facies association is represented by relative abundance of facies Cb, Gms, Sp and Scs (Table 1, Figures 6a, 7a-b). FA1 is dominated by blocky conglomerates and gravel stones. They are generally thick-bedded to massive, poorly sorted to unsorted and structureless with sharp and erosive bases and irregular tops (facies Cm and Gms). Blocky conglomerates ranging in thickness from 20 cm to 4 meters occur in FA1. They consist of angular, sub-angular and rounded clasts of marble, gneiss, schist and quartz in a calcareous matrix, with graded and pebbly imbrications locally. They can be tracked laterally for up to a hundred meters. Poorly bedded, coarse-grained pebbly sandstones (facies Sp) are generally observed as interbeds to conglomerates alternating with thin-bedded clayey sandstones (facies Scs). They can be tracked laterally for up to a few tens of meters. The clasts in the pebbly sandstones consist of marble, gneiss, schist and metagranite in a calcareous matrix. The facies has cross-bedding, symmetrical ripple marks and rare erosional bases.

FA2: The lacustrine fan delta association consists of Gms, Sp, Se, Sr, Ssh and Fs facies (Table 1, Figures 6a, 7c-d-e). The associations are commonly formed by the yellow sandstones and gray shales with evidence of localized diagenetic alteration possibly due to oxidation or mineral precipitation (facies Ssh, Sr, Se and Fs). The grain size of the sandstones varies greatly from fine to coarse sand, with mica and quartz being the dominant grains. The sandstones in the sandstone-shale interbeds have lenticular geometry and range in thickness from 10 to 30 cm. Their lateral continuity is several meters. Laminations, ripples and graded bedding are characteristics of syn-sedimentary structures. The gray shale in FA2 is between 10 and 15 cm thick. The shale beds, consisting of 1-2 cm thick laminations, contain undefined parts of coalified plants (facies Fs). The intercalation of debris-flow facies (Cb, Gms, Sp and Scs) shows an interference relationship with FA1.

Interpretation

The blocky conglomerates and gravels in FA1 were mainly deposited by debris flows with coarse-grained beds. The clasts are derived from high-grade metamorphic rocks of the Menderes Massif and cataclastic rocks of the ADF by stream debris flow processes based on the presence of angular and sub-angular clasts. The alternation of pebbly sandstones and laminated clayey sandstones indicates an area of water flow. All these facies in FA1 indicate deposition in an alluvial fan depocenter in front of a depositional area fed by the Menderes Massif.

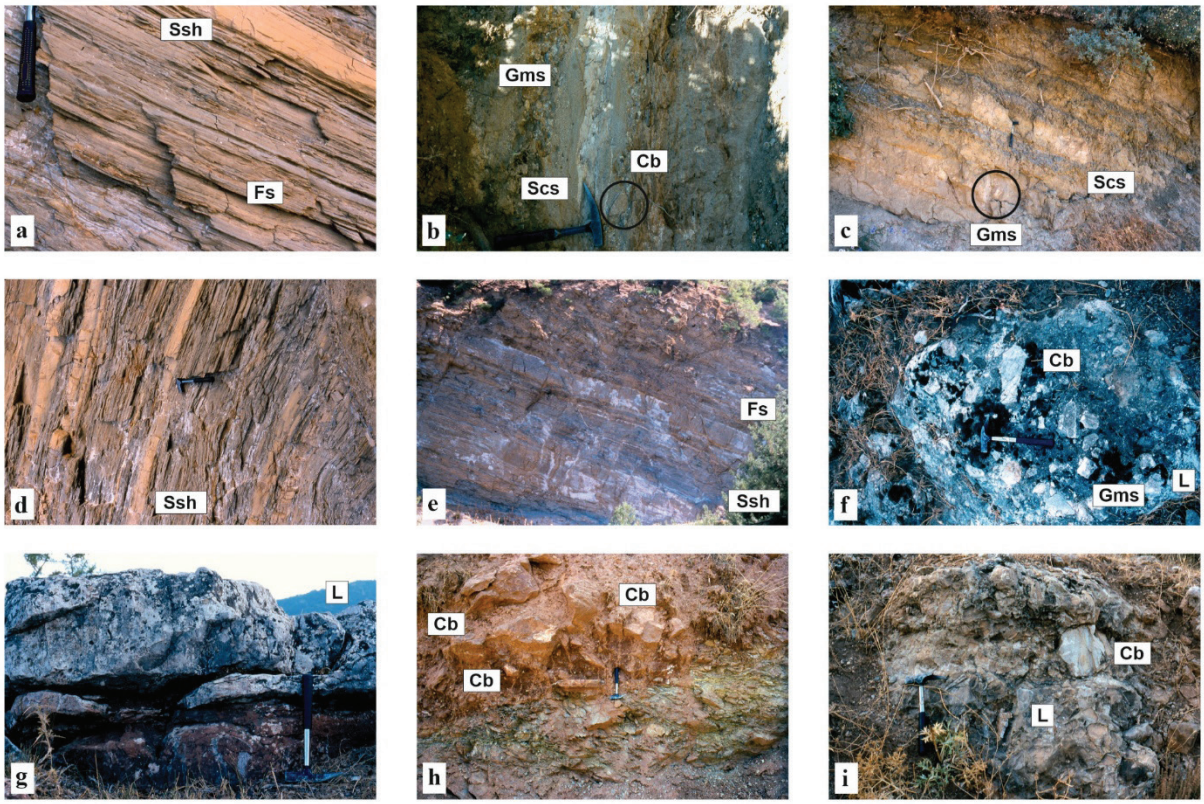

Figure 7. Outcrop views of the Lower-Middle Miocene sedimentary rocks of the Alaşehir Graben (photos taken from Şen, 2004; Ağırbaş, 2006). **(a)** Facies Fs (shales) and Ssh (alternation of sandstone and shale) consist of gray shale with yellow sandstone in the Gerentaş Formation. **(b)** Facies Cb (blocky conglomerates), Gms (gravel stones) and L (Limestones) in the Gerentaş Formation. **(c)** Facies Gms (gravel stones) and Scs (clayey sandstone) in the Gerentaş Formation. **(d-e)** Facies Ssh (alternation of sandstone-shale) and Fs (shales) in the Gerentaş Formation. **(f)** Facies Cb (blocky conglomerates) and Gms (gravel stones) are observed in the limestone bed (facies L) of the Kaypaktepe Formation, which contains angular to rounded clasts, including the cataclastic rock from the detachment fault. **(g)** The Kaypaktepe Formation consists mainly of gray limestone beds (facies L). **(h)** There are angular clasts (Cb) of cataclastic rocks above the synthetic and antithetic faults belonging to the Alaşehir detachment fault. **(i)** The limestone beds (facies L) of the Kaypaktepe Formation contain angular to sub-angular clasts (facies Cb), including Alaşehir detachment fault cataclastic rocks.

Şekil 7. *Alaşehir Grabeni' ndeki Alt-Orta Miyosen tortul kayaçlarının mostra görünümleri (Şen, 2004; Ağırbaş, 2006'dan alınan fotoğraflardır).* ***(a)*** *Gerentaş Formasyonu' nda Fs* (şeyl) ve *Ssh (kumtaşı ve şeyl ardalanması) fasiyesleri, sarı kumtaşı ile gri* şeylden *oluşmaktadır.* ***(b)*** *Gerentaş Formasyonu' nda Cb (bloklu konglomeralar), Gms* (çakıl taşları) ve L (kireçtaşları) fasiyesleri gözlenmektedir. ***(c)*** *Gerentaş Formasyonu' nda Gms* (çakıl taşları) ve *Scs (killi kumtaşı) fasiyesleri gözlenmektedir.* ***(d-e)*** *Gerentaş Formasyonu' nda Ssh (kumtaşı-şeyl ardalanması) ve Fs* (şeyl) fasiyesleri gözlenmektedir. ***(f)*** *Kaypaktepe Formasyonu'nun kireçtaşı tabakalarında (fasiyes L) fasiyes Cb (bloklu konglomeralar) ve Gms* (çakıl taşları) gözlenmektedir. Bu tabakalar, sıyrılma fayının kataklastik kayaçlarını da içeren köşeli ve yuvarlak kırıntıları içermektedir. ***(g)*** *Kaypaktepe Formasyonu esas olarak gri kireçtaşı tabakalarından (fasiyes L) oluşmaktadır.* ***(h)*** *Alaşehir sıyrılma fayına ait sintetik ve antitetik fayın üstünde kataklastik kayaçların köşeli kırıntıları (Cb) bulunmaktadır.* ***(i)*** *Kaypaktepe Formasyonu'nun kireçtaşı tabakaları (fasiyes L), Alaşehir sıyrılma fayı kataklastik kayaçlarını da içeren köşeli ve yarı köşeli kırıntıları (fasiyes Cb) içermektedir.*

The gravelly and sandy materials in FA2 were probably deposited in a lacustrine depocenter at the edge of FA1 where the alluvial fan system met the lacustrine system. Alluvial fans of FA1 facies allowed the deposition of sandstone-shale alternations due to their contact with lake water. FA2, therefore, represents deposition in the lacustrine fan delta.

The alluvial fans and fan deltas in the Gerentaş Formation are thought to result from the introduction of heavily loaded streams into a lacustrine depocenter where the lakes were small and localized as the outcrop is small (Cohen et al., 1995; İztan and Yazman, 1990; Seyitoğlu et al., 2002). However, subsurface evidence in the Alaşehir Graben suggests that lacustrine fills are more extensive (Yılmaz et al., 2000; Çiftçi and Bozkurt, 2009). The presence of angular and sub-angular clasts in blocky conglomerates and gravels in FA1 and FA2 indicates that different fragments of rock were transported into a lacustrine depocenter along alluvial fans under the control of the ADF and its synthetic and antithetic faults (Ağırbaş, 2006) (Figures 6a and 7a-e).

Kaypaktepe Formation

The Kaypaktepe Formation crops out southwest of the Alaşehir area between the villages of Soğukyurt and Gerentaş (Figure 3). The thickness of this formation is 45 meters from the measured stratigraphic log at Kaypaktepe Hill (Figure 6b), although its maximum thickness was estimated to be ~200 meters based on D-D' and E-E' cross sections (Figure 4; Ağırbaş, 2006). Seven lithofacies are described based on the nature of individual beds, grain size and primary sedimentary structures (Table 3). This lithofacies diversity is grouped into two main facies associations of FA3 (shoreline plain facies association) and FA4 (lacustrine basin facies association) (Table 2). FA3 is represented by coarse- and fine-grained beds in the lower part of the Kaypaktepe Formation and FA4 is represented by fine-grained beds in the upper part of the Kaypaktepe Formation (Figure 6b, 7f-i).

Table 3. Dominant facies, facies descriptions and interpretations for the Kaypaktepe Formation.
Çizelge 3. *Kaypaktepe Formasyonu' nun baskın fasiyesleri, fasiyes tanımları ve yorumları.*

Facies	Description	Interpretation
Cb, blocky conglomerates	Blocky conglomerates with gray silty matrix and carbonate cement, matrix-supported, poorly sorted to unsorted, chaotic, polymictic angular and sub-angular, irregular top, locally reverse and normal grading; dimensions: bed thickness up to 8 m; lateral extent tens to hundred meters	Debris flow
Gmc, matrix-supported conglomerates	Conglomerates with red calcareous matrix, poorly bedded, poorly sorted, polymictic clasts angular, sub-angular and rounded, erosive base; dimensions: bed thickness up to 2.5 m; lateral extent few tens of meters	Deposits of flash flood (channel fill)
Sp, pebbly sandstones	Coarse-grained sandstone, pebbly, poorly bedded, moderately cemented, locally fining upward with an erosive base; dimensions: bed thickness up to 20 cm; lateral extent few tens of meters	Deposits of flash flood
Sfu, fining-upward sandstones	Medium-grained sandstone, formed as a single bed, laminated, fining upward, erosive base on the bottom and ripples at top; dimensions: bed thickness up to 25 cm; lateral extent tens of meters	Subaqueous deposits at lower flow regime - waning flows
Fm, mudstones	Red color, laminated; dimensions: bed thickness up to 20 cm; lateral extent tens of meters	Low-energy (shoreline plain-lacustrine)
Fml, alternation of mudstone-limestone	Mudstone, red/gray limestone, laminated; bed thickness up to 10 cm; lateral extent tens of meters	Low-energy (lacustrine)
L, limestones	Limestone, gray color, very hard, abundant shell fragments and bioturbations; dimensions: bed thickness up to 20 cm; lateral extent tens of meters	Low-energy (lacustrine)

FA3: The shoreline plain facies association includes Cb, Gmc, Sp, Sfu and Fm facies (Table 3, Figures 6b and 7f-g). The lower and upper parts of the association consist of blocky conglomerates and matrix-supported conglomerates, ranging in thickness from 35 cm to 8 meters and from 25 to 48 cm (facies Cb and Gme). They consist of poorly sorted, rounded, angular and sub-angular clasts of dark gray black marble, gneiss, schist, quartz, meta-granite, granitoid and pebbles of breccias and cataclastic rocks together with white marble and schist. The clasts range in size from 15 cm to 1 m. All clasts are bounded by a silty matrix and carbonate cement. The middle part of the association is dominated by pebbly sandstones (facies Sp), fining-upward and rippled sandstones with an erosive base (facies Sfu) and laminated mudstones (facies Fm). Their lateral extent is usually limited to a few tens of meters.

FA4: The lacustrine basin facies association includes Gmc, Fm, Fml and L facies (Table 3, Figure 7h-i). Micaceous, tabular and laminated red mudstones (facies Fm), 10 to 20 cm thick, with limestone interbeds (facies Fml) are observed. The gray limestone, 10 to 60 cm thick, contains several undefined shell fragments and bioturbations (facies L). The lateral extent of this facies is tens of meters.

Interpretation

The alternations of coarse- and fine-grained beds in FA3 were probably deposited on the shoreline plain of a lake system. This shows periodic variations in high- and low-energy depositional processes. The association of laminated limestones and mudstones with coarse-grained clastic fills in FA4 is indicative of a lake margin depocenter. The presence of coalified plant fragments and bioturbations in the Kaypaktepe Formation suggests that its depositional setting was lacustrine, as proposed by previous researchers (İztan and Yazman, 1990; Seyitoğlu et al., 2002; Purvis and Robertson, 2005; Çiftçi and Bozkurt, 2009). The presence of rounded clasts in conglomerates indicates that different rock fragments were transported into the lake by fluvial systems, and the presence of angular and sub-angular clasts belonging to blocky conglomerates indicates that different rock fragments were transported into the lake along alluvial fans under the control of the ADF and its synthetic and antithetic faults (Ağırbaş, 2006) (Figures 6b and 7f-i).

Acıdere Formation

The Acıdere Formation is the most extensive Neogene unit along the southern margin of the Alaşehir Graben (Figure 3). The maximum thickness of the Acıdere Formation is estimated to be ~1125 meters from stratigraphic logs measured on the path along Yağmurlar to Acıdere villages and Kaynarca valley on the western part of the Ahlan Hill (Figure 8–10; Şen, 2004; Ağırbaş, 2006). Nine lithofacies are described in the Acıdere Formation (Table 4). It is a Neogene sequence consisting of alluvial and fluvial systems (Emre, 1996) and the unit is defined as a single association, including the alluvial-fan/fluvial facies association, as it is very difficult to separate these two systems (Table 2 and Figure 8–10).

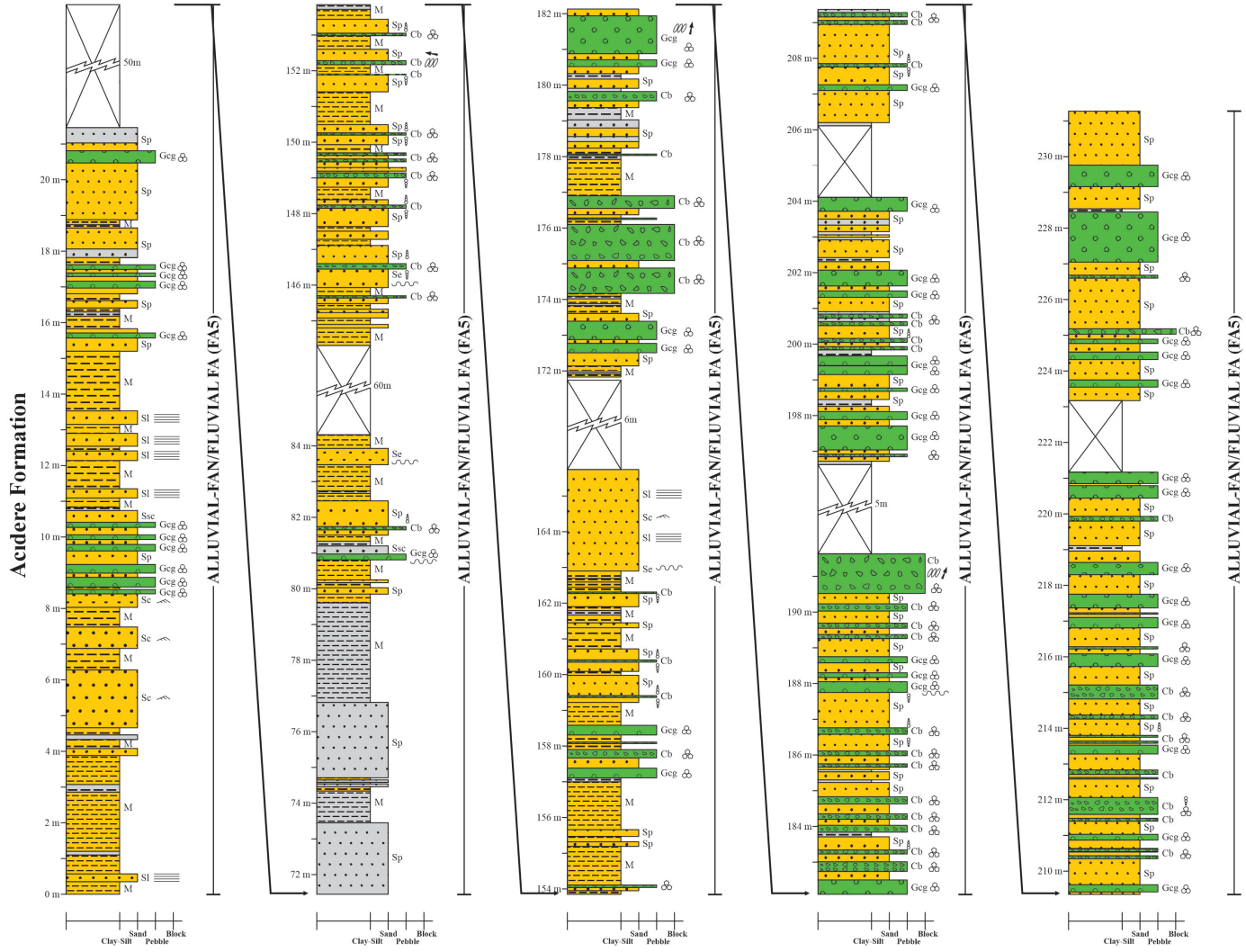

Figure 8. Measured stratigraphic log of the Acıdere Formation along the Kaynarca valley in the Alaşehir area (taken from Ağırbaş, 2006). See Figure 5 for location.

Şekil 8. *Alaşehir bölgesindeki Kaynarca Vadisi boyunca Acıdere Formasyonu' nun ölçülü stratigrafik kesiti (Ağırbaş, 2006'dan alınmıştır). Konum için Şekil 5'e bakınız.*

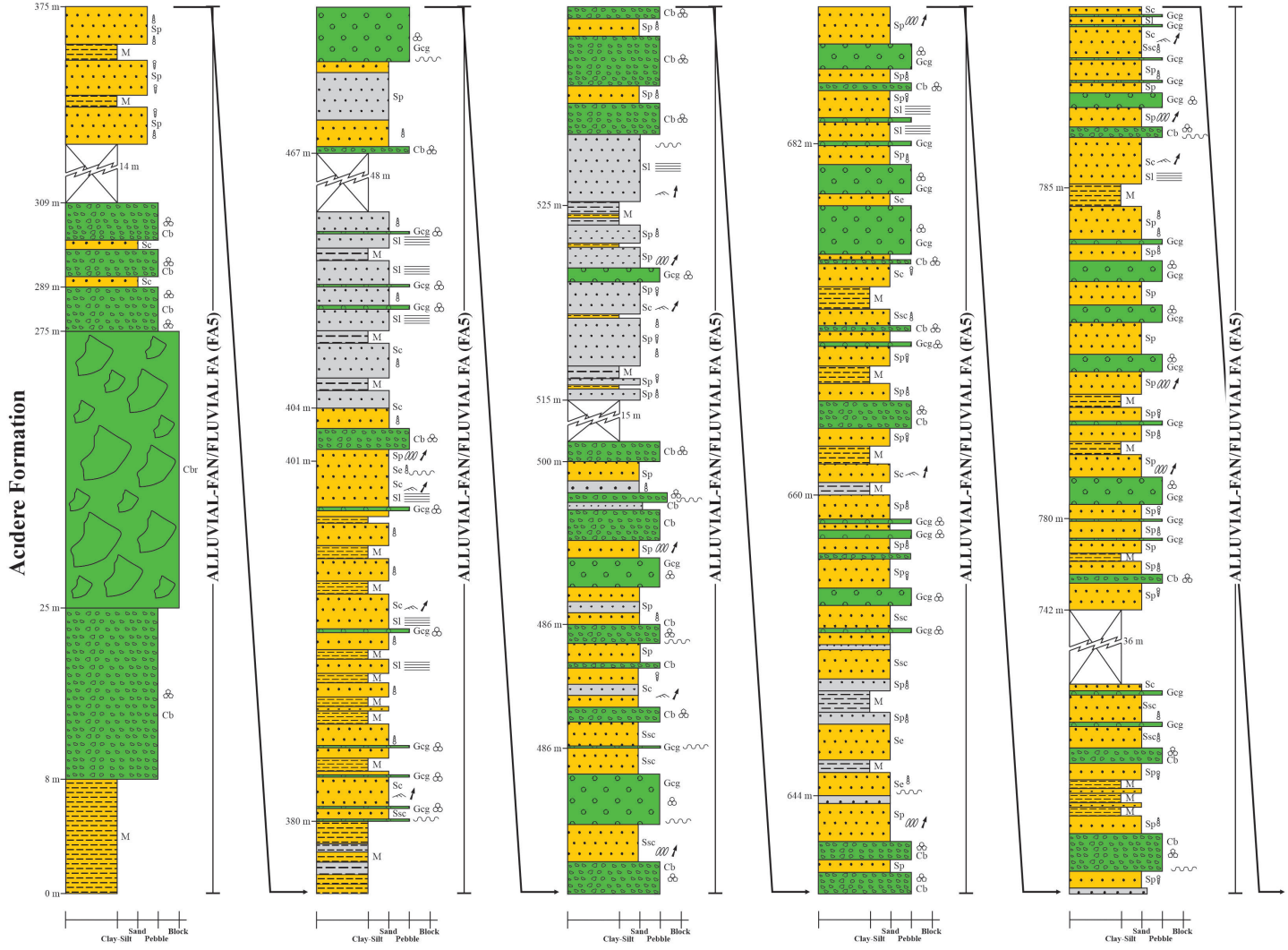

Figure 9. Measured stratigraphic log of the Acıdere Formation in the villages of Yağmurlar to Acıdere in the Salihli area (taken from Şen, 2004). See Figure 5 for location.

Şekil 9. *Salihli bölgesinde Yağmurlar' dan Acıdere' ye kadar olan köyler boyunca Acıdere Formasyonu' nun ölçülü stratigrafik kesiti (Şen, 2004'ten alınmıştır). Konum için Şekil 5'e bakınız.*

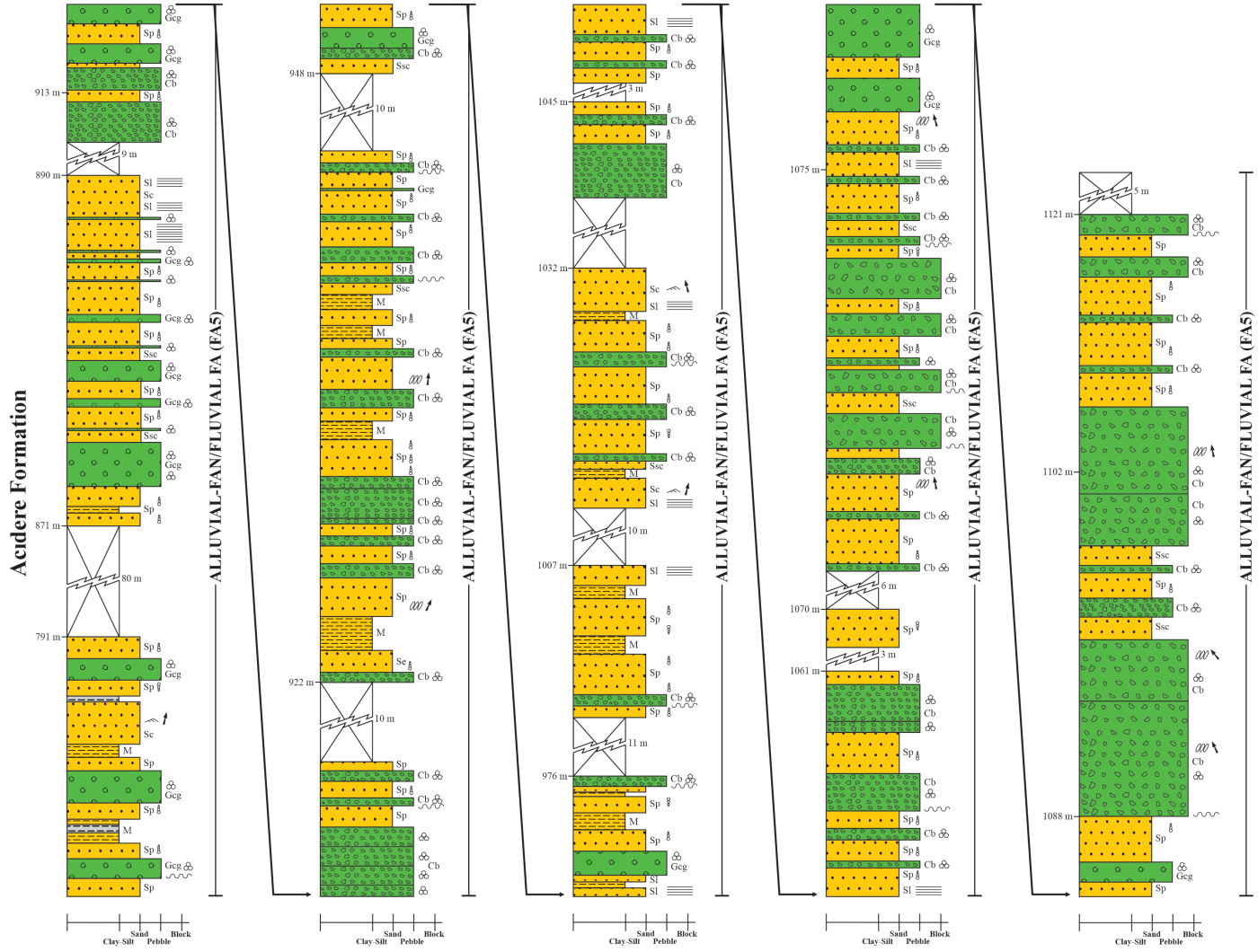

Figure 10. Measured stratigraphic log of the Acıdere Formation in the villages of Yağmurlar to Acıdere in the Salihli area (taken from Şen, 2004). Note that this is a continuation of Figure 9. See Figure 5 for location.

Şekil 10. *Salihli bölgesinde Yağmurlar' dan Acıdere' ye kadar olan köyler boyunca Acıdere Formasyonu' nun ölçülü stratigrafik kesiti (Şen, 2004'ten alınmıştır). Bunun Şekil 9'un devamı olduğunu unutmayın. Konum için Şekil 5'e bakınız.*

Table 4. Dominant facies, facies descriptions and interpretations for the Acıdere Formation.

Çizelge 4. *Acıdere Formasyonu' nun baskın fasiyesleri, fasiyes tanımları ve yorumları.*

Facies	Description	Interpretation
Cb, blocky conglomerates	Blocky conglomerates with red sandy to gravelly matrix, matrix-supported, chaotic, poorly sorted, polymictic angular and sub-angular clasts, irregular top, pebbly imbrications; dimensions: bed thickness up to 5 m; lateral extent tens to hundred meters	Debris flow
Cbr, breccias	Breccias, blocks and gravel stones of breccias from the Alaşehir detachment fault, poorly sorted, angular clasts; dimensions: bed thickness up to 10 m; lateral extent tens to hundred meters	Debris flow
Gcg, cross-bedded gravel stones and conglomerates	Gravelstones and conglomerates with red sandy matrix and granule to pebble size clasts supported by coarse sand matrix, poorly sorted, moderately cemented, polymictic, erosive base, cross-bedding; dimensions: bed thickness up to 1 m; lateral extent few tens of meters	Channel fills
Sp, pebbly sandstones	Coarse-grained sandstones with red and gray silty matrix, pebbly, poorly sorted, moderately cemented, erosive base; dimensions: bed thickness up to 1 m; lateral extent few tens of meters	Deposits of flash flood - channel fills
Sc, cross-bedded sandstones	Medium- and fine-grained sandstones, red and gray color, good to moderate sorting, cross-bedding; dimensions: bed thickness up to 40 cm; lateral extent few tens of meters	Crevasse splays
Se, erosive-based sandstones	Coarse-grained sandstones, red and gray colored, good to moderate sorting, erosive based with cross-bedding and normal and reverse grading; dimensions: bed thickness up to 40 cm; lateral extent few less than 20 meters	Scour-fills
Ssc, scoured-based sandstones	Coarse-grained sandstones, red and gray color, good to moderate sorting, broad scoured based with lag, fining upward; dimensions: bed thickness up to 40 cm; lateral extent less than 10 meters	Scour-fills
Sl, laminated sandstones	Coarse- and fine-grained sandstones, well sorted, laminated; dimensions: bed thickness up to 40 cm; lateral extent few tens of meters	Deposits from planar bed flow-waning currents in channel
M, mudstones	Mudstones, red and gray color, laminated; dimensions: bed thickness up to 30 cm; lateral extent few tens of meters	Waning currents in channel

FA5: The alluvial-fan/fluvial facies association is composed of Cb, Cbr, Gcg, Sp, Sc, Se, Ssc, Sl and M facies (Table 4; Figures 8–11). The facies association is dominated by blocky conglomerates and gravel stones (facies Cb, Cbr and Gcg) with intercalations of sandy facies (Sp, Sc, Se, Ssc and Sl), including well to poorly-sorted, moderate- to well-cemented sandstones alternating with mudstones (facies M). Blocky conglomerates and conglomerates are characteristically red, poorly sorted, with pebble imbrications, angular to sub-angular clasts containing quartz, marble, gneiss, schist, granitoid, meta-granite and cataclastic rocks. Clasts range in size from 0.3 cm to 1 m. Bed thicknesses range from 1 to 5 meters (Figures 8–10, 11a-c). The sandstone beds are matrix-supported in the lower part and grain-supported in the upper part of FA5. The sandstone is moderately well sorted, with normal-reverse graded, cross-bedding, and contains rounded small clasts of quartz, marble, gneiss, schist, granitoid, meta-granite, and cataclastic rocks in a carbonate matrix. The pebbles in the sandstone contain moderately poorly sorted, angular, sub-angular and rounded clasts, consisting of quartz, marble, gneiss, schist, granitoid, meta-granite and cataclastic rocks, and clast sizes range from 0.3 to 15-20 cm (Figures 8–10, 11d-i). Thicknesses range from 40 cm to 2 meters. The mudstones are 20 to 40 cm thick (Figure 8–10). They are red and locally gray. The gray color is usually observed in the gravelly and sandy facies.

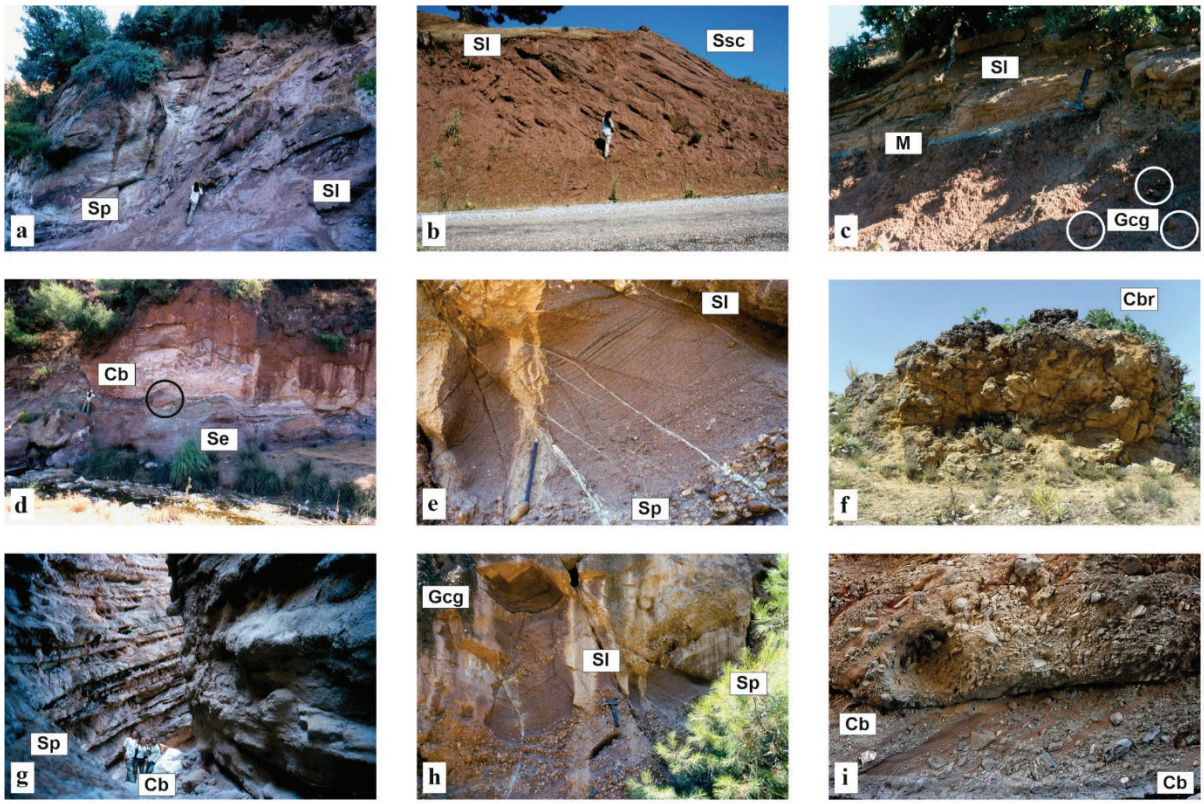

Figure 11. Outcrop views of the Lower-Upper Miocene sedimentary rocks of the Alaşehir Graben (photos taken from Şen, 2004; Ağırbaş, 2006). **(a)** Facies Sp (pebbly sandstones) and Sl (laminated sandstones) in the Acıdere Formation. **(b)** Facies Sl (laminated sandstones) and Ssc (sandstones) in the Acıdere Formation. **(c)** Facies Gcg (gravel stones and conglomerates), Sl (laminated sandstones) and M (mudstones) in the Acıdere Formation. **(d)** Facies Cb (blocky conglomerates) and Se (erosive-based sandstones) in the Acıdere Formation. **(e-f)** Facies Sp (pebbly sandstones) and Sl (laminated sandstones) in the Acıdere Formation. **(g)** The Acıdere Formation consists mainly of Cb facies (blocky conglomerates) and Sp (pebbly sandstones) in the Kaynarca valley. **(h-i)** The sandstone beds of the Acıdere Formation in the Kısık valley contain angular to rounded clasts (facies Cb, Gcg and Sp), including cataclastic rock from the Alaşehir detachment fault.

Şekil 11. *Alaşehir Grabeni' nin Alt-Üst Miyosen tortul kayaçlarının mostra görünümleri (Şen, 2004; Ağırbaş, 2006'dan alınan fotoğraflardır).* ***(a)*** *Acıdere Formasyonu'nda Sp (çakıllı kumtaşları) ve Sl (laminalı kumtaşları) fasiyesleri gözlenmektedir.* ***(b)*** *Acıdere Formasyonu'nda Sl (laminalı kumtaşları) ve Ssc (kumtaşları) fasiyesleri gözlenmektedir.* ***(c)*** *Acıdere Formasyonu'nda Gcg* (çakıl taşı ve konglomeralar), *Sl (laminalı kumtaşları) ve M (çamurtaşları) fasiyesleri gözlenmektedir.* ***(d)*** *Acıdere Formasyonu'nda Cb (bloklu konglomeralar) ve Se (aşındırıcı tabanlı kumtaşları) fasiyesleri gözlenmektedir.* ***(e-f)*** *Acıdere Formasyonu'nda Sp (çakıllı kumtaşları) ve Sl (laminalı kumtaşları) fasiyesleri gözlenmektedir.* ***(g)*** *Kaynarca Vadisi'ndeki Acıdere Formasyonu çoğunlukla Cb (bloklu konglomeralar) ve Sp (çakıllı kumtaşları) fasiyeslerden oluşur.* ***(h-i)*** Kısık Vadisi› *ndeki Acıdere Formasyonu'nun kumtaşı katmanları, Alaşehir sıyrılma fayının kataklastik kayacı da dahil olmak üzere köşeli ve yuvarlak kırıntıları (fasiyes Cb, Gcg ve Sp) içermektedir.*

Interpretation

The alternations of coarse- and fine-grained beds in FA5 were probably deposited in the fluvial depocenter under the control of alluvial-fan systems (Emre, 1996). The predominantly channeled appearance of the sandstones and conglomerates is texturally immature. This suggests a high-energy depocenter in the form of longitudinal and transverse bars in a braided river system (e.g., Emre, 1996; Purvis and Robertson, 2005; Çiftçi and Bozkurt, 2009). The alluvial fans were fed from south to north by the Menderes Massif and prograded northwards towards the Miocene graben, where they drained into river systems.

The lowermost part of the Acıdere Formation begins with sandy beds alternating with muddy beds on the Alaşehir side, while the lowermost part of this unit begins with blocky and gravelly beds on the Salihli side ((Figures 8–10 and 11). The depositional age of the middle and upper levels of the Acıdere Formation is middle to late Miocene based on an Eskihisar sporomorph association and some palynological fauna (Ediger et al., 1996; Seyitoğlu and Scott, 1996). The blocks containing large breccia from the ADF in the lower parts of this deposit on the Salihli side correspond to blocky conglomerates composed of breccias on the detachment fault in the lower parts of the Kaypaktepe Formation in the Alaşehir area. These breccias provide a reference level for comparison between the two units. Thus, the age of the Acıdere Formation is Lower-Upper Miocene (Şen, 2004; Şen et al., 2024).

Deposition in the Salihli area took place in an alluvial-fan environment based on the presence of blocks with large breccias belonging to the ADF, while sedimentation in the lacustrine environment continued in the Alaşehir area during the Early to Middle Miocene. The lacustrine depocenter for the Gerentaş and Kaypaktepe Formations is not observed in the Acıdere Formation due to the presence of mudstone and sandstone with conglomerate interlayers in the upper parts of this unit in the Alaşehir area. The lakes fed by the rivers were filled with sediments from the Gerentaş and Kaypaktepe Formations. As a result, material carried by the rivers never reached a lacustrine depocenter and was deposited as fluvial fills in the Alaşehir area. The presence of pebble imbrications in the conglomerate beds and normal-reverse gradations, together with cross-bedding in the sandstone beds, indicate that its depocenter is in a fluvial system, as stated by Dunbar and Rodgers (1957) and Önalan (1997). Furthermore, the presence of angular and sub-angular clasts and pebble imbrications in the conglomerate beds and conglomerate-sandstone intercalations show that different rock fragments were transported into the fluvial systems along alluvial fans under the control of the ADF and its synthetic-antithetic faults (Şen, 2004; Ağırbaş, 2006).

Göbekli Formation

The Göbekli Formation is exposed southeast of the Salihli area between the villages of Göbekli and Kurudere and south of the village of Yağmurlar and north of the village of Peynirçukuru (Figure 3). The thickness of the unit is ~585 meters according to the measured stratigraphic log along the Koğukdere valley (Figure 12–14a; Şen, 2004, 2016). Eleven lithofacies are defined in the Göbekli Formation (Table 5). This lithofacies diversity is divided into two main facies associations of FA6 (alluvial-fan/fluvial facies association) and FA7 (floodplain facies association) (Table 2). FA6 refers to the dominant coarse-grained beds in the lower levels of the Göbekli Formation, and FA7 refers to the dominant fine-grained beds in its middle and upper levels.

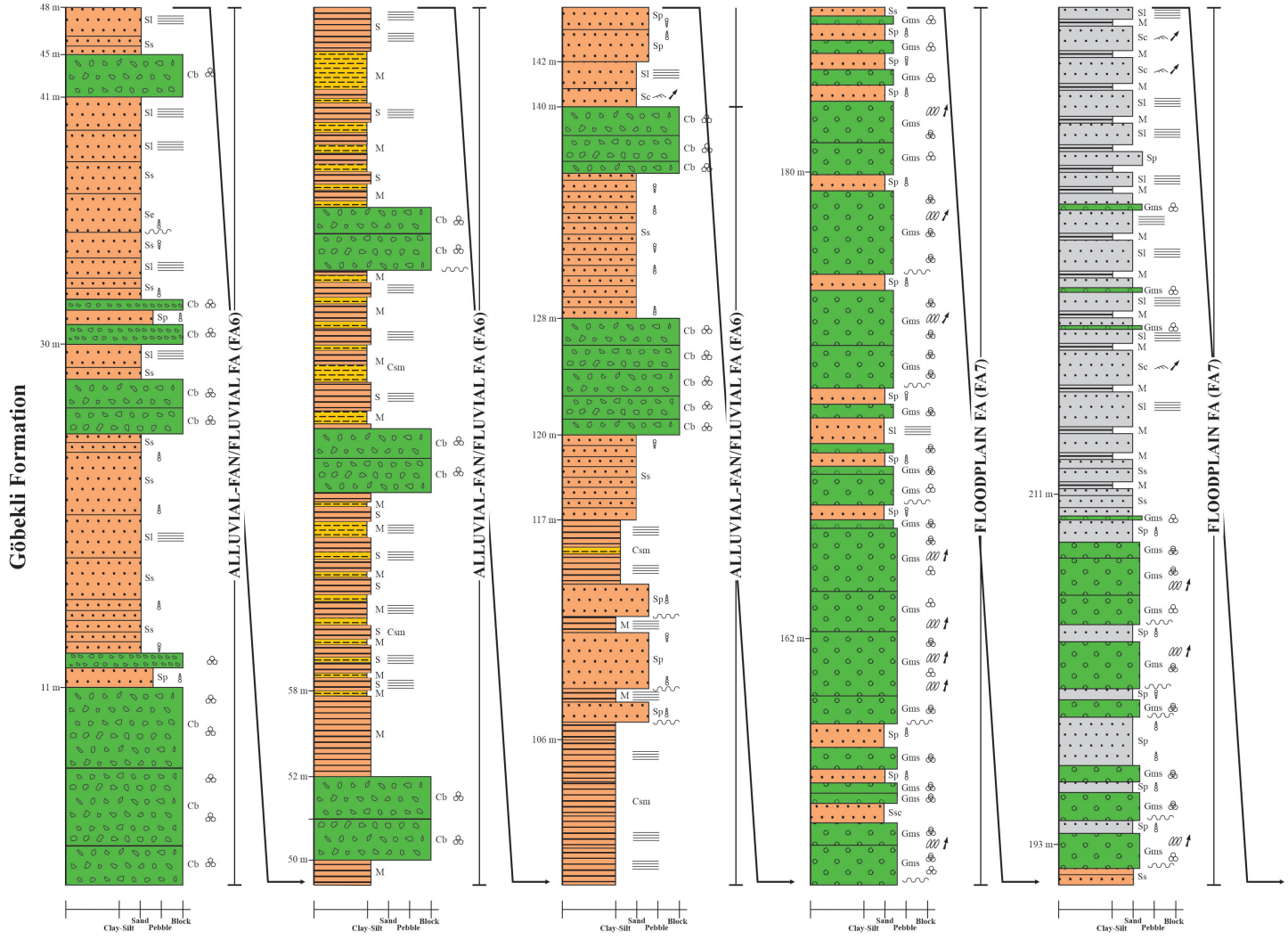

Figure 12. Measured stratigraphic log of the Göbekli Formation along the Koğukdere valley in the Salihli area (taken from Şen, 2004). See Figure 5 for location.

Şekil 12. *Salihli bölgesindeki Koğukdere Vadisi boyunca Göbekli Formasyonu'nun ölçülü stratigrafik kesiti (Şen, 2004'ten alınmıştır). Konum için Şekil 5'e bakınız.*

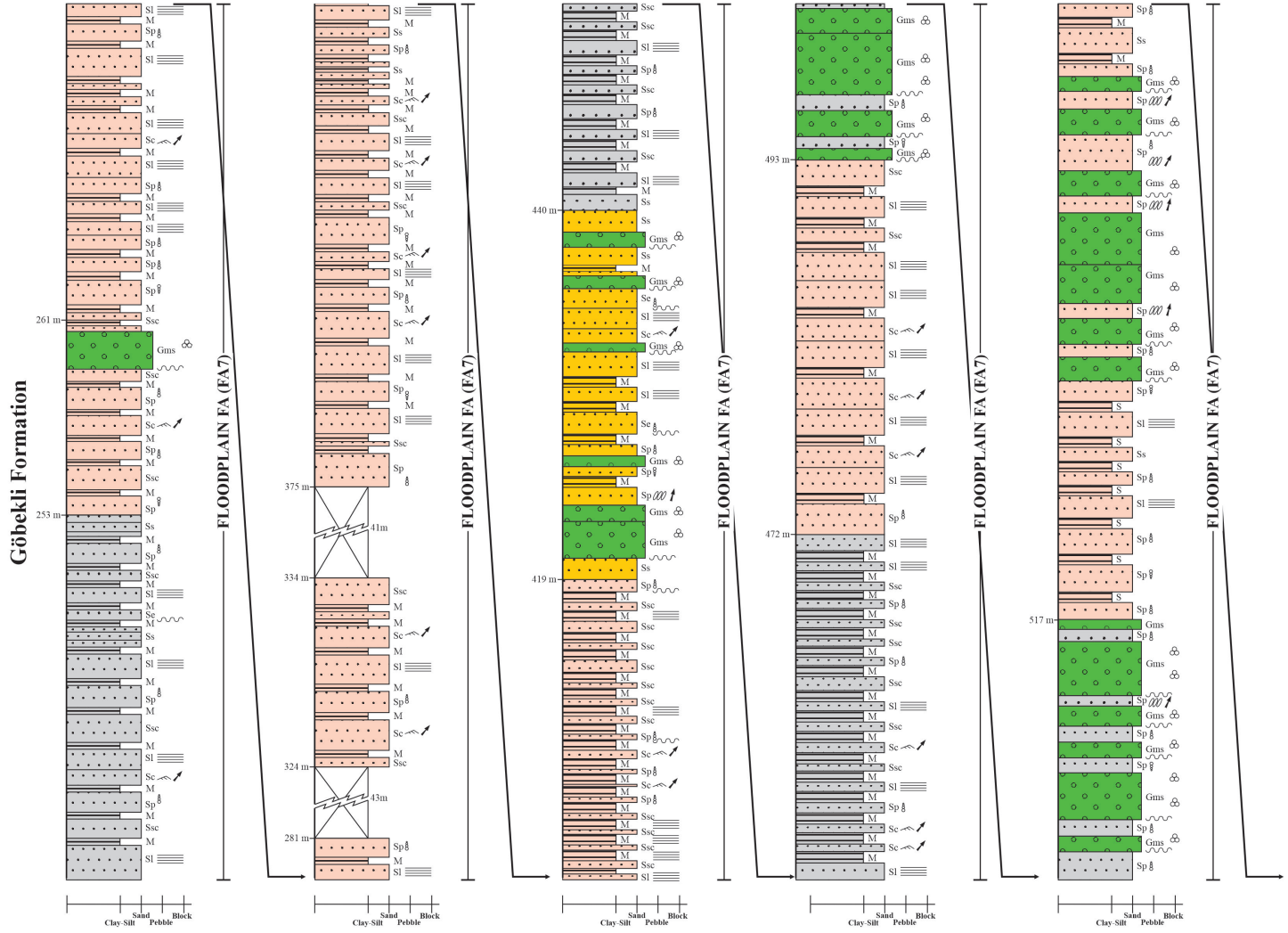

Figure 13. Measured stratigraphic log of the Göbekli Formation along the Koğukdere valley in the Salihli area (taken from Şen, 2004). Note that this is a continuation of Figure 12. See Figure 5 for location.

Şekil 13. *Salihli bölgesindeki Koğukdere Vadisi boyunca Göbekli Formasyonu'nun ölçülü stratigrafik kesiti (Şen, 2004'ten alınmıştır). Bunun Şekil 12'nin devamı olduğunu unutmayınız. Konum için Şekil 5'e bakın.*

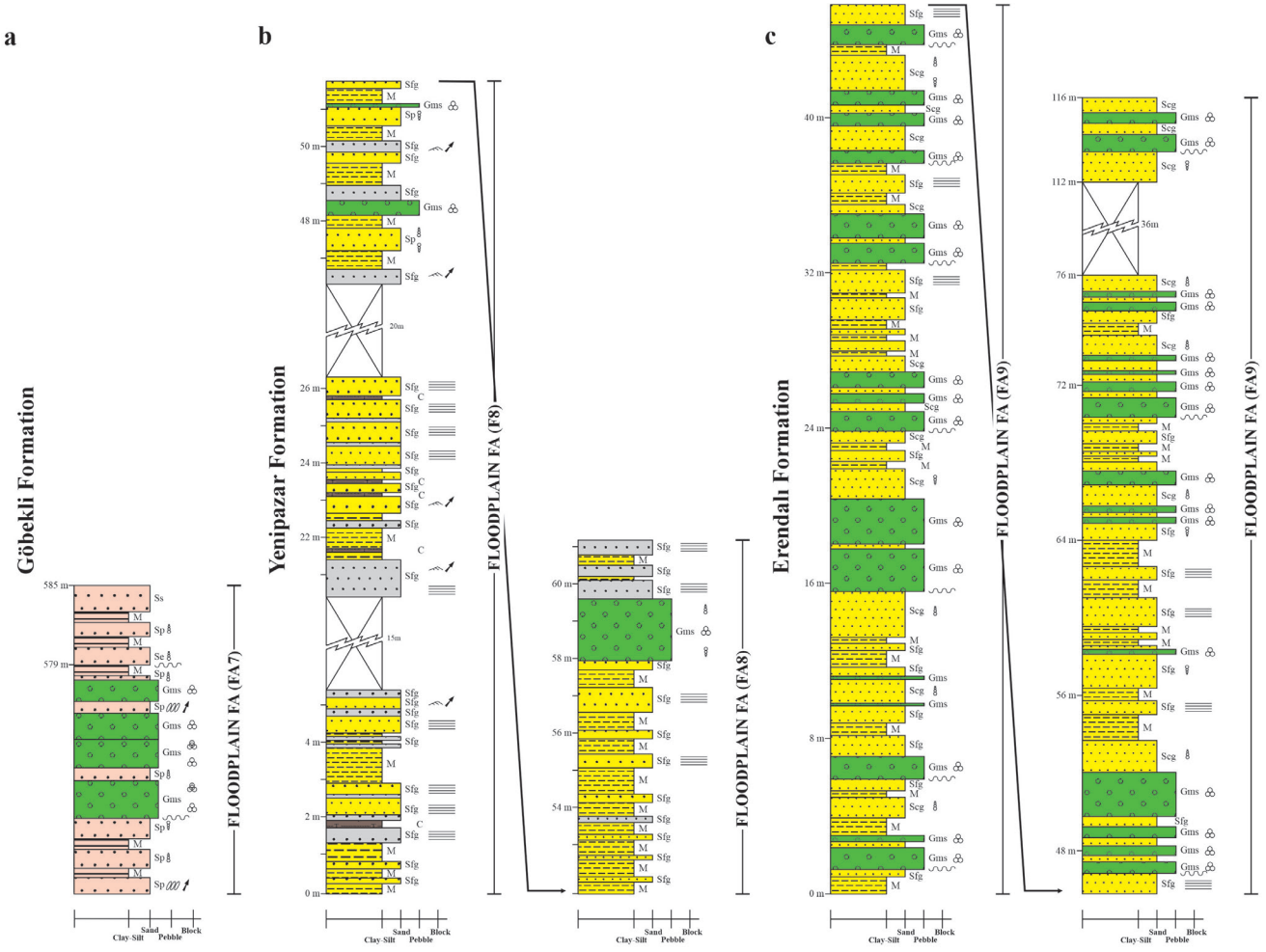

Figure 14. Measured stratigraphic log of the Göbekli Formation along the Koğukdere valley **(a)** and the Erendalı Formation on Erendalı Hill **(b)** in the Salihli area (taken from Şen, 2004) and the Yenipazar Formation along the Kokar valley **(c)** in the Alaşehir area (taken from Ağırbaş, 2006). Note that Figure 14a is a continuation of Figure 13. See Figure 5 for location.

Şekil 14. *Salihli yöresinde Koğukdere Vadisi boyunca Göbekli Formasyonu'nun* ***(a)*** *ve Erendalı Tepesi'nde Erendalı Formasyonu'nun (b) (Şen, 2004'ten alınmıştır) ve Alaşehir yöresinde Kokar Vadisi boyunca Yenipazar Formasyonu'nun* ***(c)*** *ölçülü stratigrafik kesitleri (Ağırbaş, 2006'dan alınmıştır). Şekil 14a'nın Şekil 13'ün devamı olduğunu unutmayın. Konum için Şekil 5'e bakınız.*

Table 5. Dominant facies, facies descriptions and interpretations for the Göbekli Formation.
Çizelge 5. Göbekli Formasyonu'nun *baskın fasiyesleri, fasiyes tanımları ve yorumları.*

Facies	Description	Interpretation
Cb, blocky conglomerates	Blocky conglomerates with yellow color silty matrix and carbonate cement, matrix-supported, poorly sorted to unsorted, chaotic, polymictic angular and sub-angular clasts; dimensions: bed thickness up to 11 m; lateral extent tens to hundred meters	Debris flow
Gms, matrix-supported gravel stones	Gravel stones with yellow, gray, red, and pink silty matrix and carbonate cement, matrix-supported, sorted, polymictic sub-rounded to rounded clasts, erosive based, pebble imbrications; dimensions: bed thickness up to 5 m; lateral extent few tens of meters	Channel fills
Sp, pebbly sandstones	Coarse- and fine-grained sandstones with yellow, gray, red, and pink silty matrix and carbonate cement, matrix-supported, moderately well-sorted, normal to reverse graded; dimensions: bed thickness up to 6 m; lateral extent few tens of meters	Deposits of flash flood/ channel deposits
Se, erosive-based sandstones	Coarse- and fine-grained sandstones with yellow, gray, red, and pink silty matrix and carbonate cement, matrix-supported, moderately well-sorted, erosive-based, locally normal graded; dimensions: bed thickness up to 1 m; lateral extent few less than ten meters	Scour-fills/channel fills and sand bars
Sc, cross-bedded sandstones	Medium- to fine-grained sandstones, yellow, gray, red, and pink color, moderately well-sorted, tabular cross-bedded; dimensions: bed thickness up to 1.2 m; lateral extent few tens of meters	Sand bars
Sl, laminated sandstones	Medium- to fine-grained sandstones, horizontally laminated; dimensions: bed thickness up to 50 cm; lateral extent several tens of meters	Planar bed flow deposits
Ss, stratified sandstones	Medium- to fine-grained sandstones, moderately sorted, locally laminated; dimensions: bed thickness up to 60 cm; lateral extent few tens of meters	Waning flood deposits
Ssc, clayey-silty sandstones	Sandstones with clayey and silty, well-sorted, locally laminated	Waning flood deposits
Csm, alternation of siltstone–mudstone	Siltstones and mudstones, laminated; bed thickness up to 20 cm; lateral extent several tens of meters	Waning currents in channel
S, siltstones	Siltstones, laminated, locally sandy; dimensions: bed thickness up to 30 cm; lateral extent tens of meters	Waning currents in channel
M, mudstones	Mudstones, locally laminated; dimensions: bed thickness up to 60 cm; lateral extent several tens of meters	Waning currents in channel/overbank

FA6: The alluvial-fan/fluvial facies association includes Cb, Sp, Ss, Sl, Se, S, M and Csm facies (Table 5; Figure 12). The dominant facies of this association is blocky conglomerate (facies Cb). The lower and upper parts of the association are dominated by sandy facies (Sp, Ss, Sl and Se); however, the sandy facies is replaced by siltstone-mudstone facies in the middle part of the association (facies Csm, S and M). Blocky conglomerates are observed in FA6 (Figure 12, 15d-f). They consist of angular to sub-angular clasts of marble, gneiss, metagranite, schist, granitoid, cataclastic rocks, and reworked fragments of the Acıdere Formation. The clasts range in size from 0.1 cm to 1 m. All clasts are bounded by a silty matrix and carbonate cement. Bed thickness ranges from 1 to 11 meters. The shape and origin of the pebbles in the pebbly sandstones of the association are the same as in the blocky conglomerates.

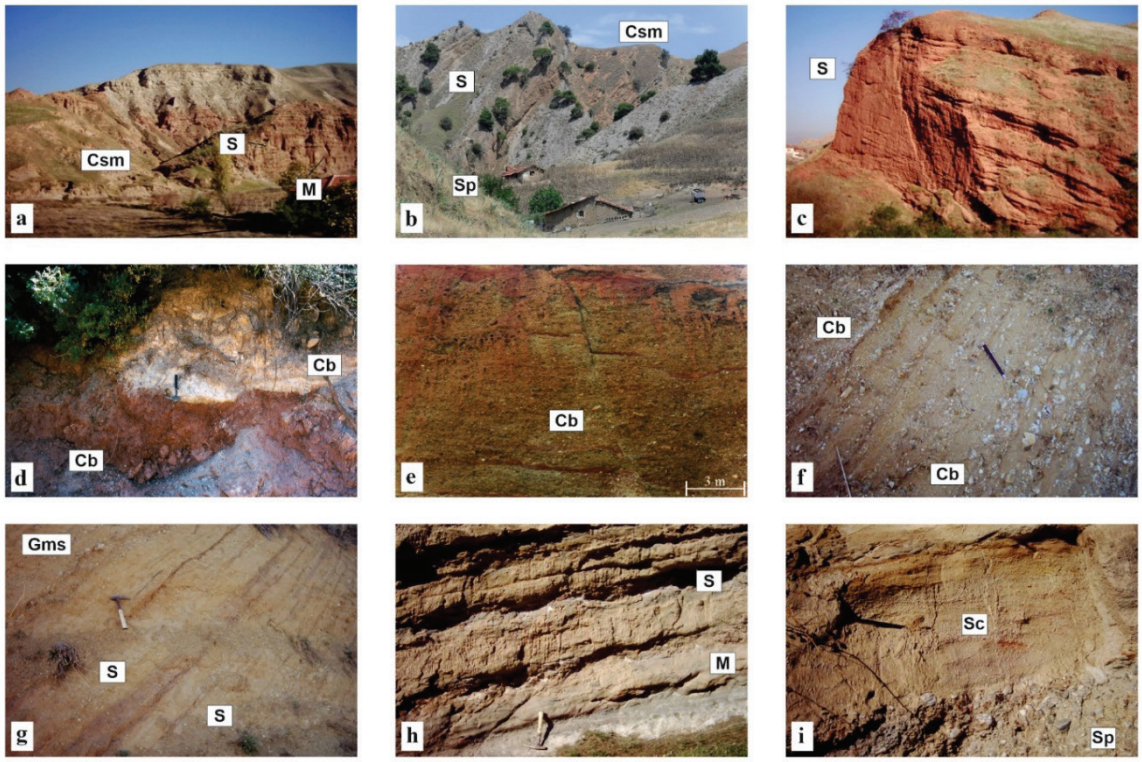

Figure 15. Outcrop views of the Upper Miocene-Upper Pliocene sedimentary rocks of the Alaşehir Graben (photos taken from Şen, 2004; Ağırbaş, 2006). **(a-c)** Facies Csm (alternation of siltstone–mudstone), S (siltstones), M (mudstones) Sp (pebbly sandstones) and S (stratified sandstones) in the Göbekli Formation. **(d)** There are angular clasts (facies Cb), including cataclastic rocks of the Alaşehir detachment fault, in the first 7 meters level of the Göbekli Formation overlying the Acıdere Formation, and **(e)** there are angular to sub-angular clasts (facies Cb, including cataclastic rocks from the Alaşehir detachment fault in the first 140 meters in the Koğukdere valley. **(f)** There are angular to sub-angular clasts (facies Cb), including cataclastic rocks from the Alaşehir detachment fault between 7 and 140 meters; but the size of the clasts belonging to the cataclastic rocks is quite small compared to the sizes in the first 7 meters. **(g)** There are interbeds of fine- and coarse-grained sandstones (facies S) consisting of rounded clasts (facies Gms) lacking cataclastic rocks of the Alaşehir detachment fault. **(h)** Facies S (sandstones) and M (mudstones) in the Göbekli Formation. **(i)** Facies Sp (pebbly sandstones) and Sc (cross-bedded sandstones) in the Göbekli Formation after the first 140 meters and the sphericity of the pebbles in the sandstone beds is sub-rounded to rounded.

Şekil 15. *Alaşehir Grabeni'nin Üst Miyosen-Üst Pliyosen tortul kayaçlarının mostra görünümleri (fotoğraflar Şen, 2004; Ağırbaş, 2006'dan alınmıştır).* ***(a-c)*** Göbekli Formasyonu'*nda Csm (siltaşı-çamurtaşı ardalanması), S (siltaşı), M (çamurtaşı), Sp (çakıllı kumtaşı) ve S (tabakalı kumtaşı) fasiyesleri gözlenmektedir.* ***(d)*** *Acıdere Formasyonu üzerinde yer alan Göbekli Formasyonu'nun ilk 7 metrelik seviyesinde, Alaşehir sıyrılma fayının kataklastik kayaçlarını da içeren köşeli kırıntılılar (fasiyes Cb) ve* ***(e)*** *Koğukdere Vadisi'nde ilk 140 metrelik seviyede, Alaşehir sıyrılma fayının kataklastik kayaçlarını da içeren köşeli ve yarı köşeli kırıntılar (fasiyes Cb) bulunmaktadır.* ***(f)*** *7 ile 140 metre seviyeleri arasında, Alaşehir sıyrılma fayının kataklastik kayaçlarını da içeren köşeli ve yarı köşeli kırıntılılar (fasiyes Cb) bulunmaktadır; ancak kataklastik kayaçlara ait kırıntıların boyutu ilk 7 metredeki boyutlara göre oldukça küçüktür.* ***(g)*** *Yuvarlak kırıntılılardan (fasiyes Gms) oluşan, ince- ve kaba-taneli kumtaşları (fasiyes S) ara katmanları.* ***(h)*** Göbekli Formasyonu'nda S (kumtaşı) ve M (çamurtaşı) fasiyesleri gözlenmektedir. ***(i)*** *Göbekli Formasyonu'nda ilk 140 metreden sonra Sp (çakıllı kumtaşı) ve Sc (çapraz katmanlı kumtaşı) fasiyesleri gözlenmekte olup, kumtaşı katmanlarındaki çakılların küreselliği yarı yuvarlaktan yuvarlağa doğrudur.*

FA7: The floodplain facies association is composed of Gms, Sp, Se, Sc, Sl, SS, Ssc, Csm, S and M facies (Table 5; Figures 12-14a, 15a-c). The facies association is dominated by gravel stones (facies Gms) with sandy facies (Sp, Se, Sc, Ss and Ssc) consisting of well to poorly sorted, moderate- to well-cemented sandstones alternating with siltstones and mudstones (facies Csm, S and M). Gravel stones contain sub-rounded to rounded clasts including rock fragments from the high-grade metamorphic rocks and from the Gerentaş, Kaypaktepe and Acıdere Formations. The clasts range from 0.1 cm to 6 cm in size. They are bounded by a silty matrix and carbonate cement. Bed thickness ranges from 50 cm to 5 meters. The shape and origin of the clasts in the pebbly sandstones of FA7 are the same as in the gravels. The clast geometry is round in pebble and gravel sandstones in FA7 (Figures 12–14a, 15). The sandy facies contains moderately well sorted, normal to reverse graded, cross-bedded and pebble imbrications, with rounded clasts of quartz, marble, schist, and gneiss in a carbonate matrix. Thicknesses range from 2 cm to 6 m. Erosional structures are observed between coarse- and fine-grained beds (Figure 15g). The muddy and silty facies are interbedded with sandy facies (Figure 7g-i). Bed thickness is 50-60 cm (Figure 15h-i). The sedimentary rocks are yellow, gray, red and pink, and show lateral and vertical repetition at varying intervals in FA7 (Figures 12–14a, 15).

Interpretation

The depocenter where the Göbekli Formation was formed is a floodplain (Emre, 1996). Floodplain deposits are represented by a continuum of fill types, ranging from clay- to gravel-sized particles and including both terrigenous and organic fills. The shape of pebbles deposited in floodplain sedimentary rocks ranges from sub-rounded to rounded. Floodplain deposits consist of channel deposits and overbank deposits associated with seasonal increases in river flow caused by prolonged periods of snowmelt and excessive rainfall (Gerard, 2003; Bølviken et al., 2004). However, the Göbekli Formation was deposited in two different depocenters, represented by alluvial-fan/fluvial (FA6) and floodplain (FA7) associations.

The alternation of coarse- and fine-grained beds in FA6 was probably deposited in the fluvial depocenter under the control of alluvial-fan systems. FA6 represents the first 140 meters of the Göbekli Formation. The presence of angular to sub-angular clasts of blocky conglomerate in the first 140 meters of the Göbekli Formation supports an alluvial-fan origin during an early stage of deposition (Figure 15d-f). The presence of normal-reverse graded, cross-bedding, and pebble imbrications in the pebbly sandstones in beds between 12 and 140 meters indicates a fluvial depocenter in the later levels of the sequence (Figure 12). The first 140 meters of the sequence formed as a result of transport to fluvial systems along the alluvial-fans above the Acıdere Formation. After the first 140 meters (FA6), the presence of lenses and normal- to reverse-graded pebbles in gravel stone, pebbly sandstone and fine-grained sandstone beds indicates a low-energy depocenter (Figure 15g-i). There are also repeated erosional basal structures above the fine-grained sandstone beds after the first 140 meters. This indicates that these beds are channel deposits (Figures 12–14a and 15a, b). Channel deposits, consisting of channel-bar and channel-fill sediments with normal-reverse grading, cross-beddings and pebble imbrications, are dominated by coarse-grained fills such as sand and gravel. Channel-bar sediments are typically stratified sands and gravels and accumulate in response to river migration and changes in river systems. Channel-fill sediments range from coarse- to fine-grained deposits. There is a recurrent pattern of erosional base structures between the channel bar and fill sediments (Fisk, 1947; Gerard, 2003;

Bølviken et al., 2004). After this level, there are layers of mudstone and sandstone alternating with siltstone. This is indicative of low-dipping morphology. This means that these levels are overbank deposits (Figures 12–14a and 15a-b, i). Overbank deposits are fine-grained and accumulate vertically, consisting mainly of mud, silt, and lesser amounts of sand, and organic sediments, such as lignite and bituminous coal horizons, are important constituents in floodplains. They occur along rivers and streams with variable discharge. They are deposited on floodplains and embankments by the suspension of water during floods when the discharge exceeds what can be contained in the normal channel (Flores, 1981, Bølviken et al., 2004).

This clearly shows that the Göbekli Formation continues as a series of successive packages, resulting in a more monotonous sequence after the first 140 meters (Figure 12–14a) and the depositional environment of the Göbekli Formation is clearly identified as a floodplain setting within the Alaşehir Graben.

The blocky conglomerates and pebbles in the pebbly sandstone beds of the first 140 meters of the Göbekli Formation were formed in fluvial systems along alluvial fans under the influence of tectonic activity on the ADF and its synthetic and antithetic normal faults during the late Miocene (Şen, 2004, 2016). This is because the shapes of the pebbles are sub-rounded and round, and there are no more angular cataclastic pebbles after this level. This means that this sequence, except for the first 140 meters, was deposited in flat plain deposits without any tectonic activity on the ADF during the latest late Miocene to latest early Pliocene.

Yenipazar Formation

The Yenipazar Formation is exposed southwest of the Salihli and Alaşehir areas in the villages of Kaysanlı[2], Yeşilkavak and Yeniköy (Figure 3). The thickness of the Yenipazar Formation is 62 m from the measured stratigraphic log in the Kokar Valley (Figure 14b), although its maximum thickness has been estimated to be ~350 m based on B-B' and C-C' cross sections (Figure 4; Şen, 2004; Ağırbaş, 2006). Five lithofacies are described in the Yenipazar Formation, including FA8 (floodplain facies association) (Tables 2 and 6). FA8 refers to the predominance of fine-grained beds with a minor presence of coarse-grained beds.

FA8: The floodplain facies association consists of Gms, Sp, Sfg, M and C facies (Table 6; Figure 14b). The facies association is dominated by gravel stones (facies Gms) with sandy facies (Sp and Sfg), containing gray mudstones (facies M) alternating with lignite and bituminous coal horizons (C) in the lower part of the association (Figure 14b, 16a-c). The gravel stones in FA8, ranging in size from 1 to 5 cm, consist of sub-rounded and rounded clasts of high-grade metamorphic rocks in a calcareous matrix. Bed thickness ranges from 40 cm to 3 meters. The shape and origin of the pebbles in the pebbly sandstones are the same as those in the gravel stones. The fine-grained sandstones (facies Sfg) contain moderately to poorly consolidated, thin to medium bedded, and poorly sorted clastics alternating with mudstones (facies M) and exhibits cross-bedding and laminations. Pedogenic slickensides are abundant in the organic-bearing muddy beds (Figure 15c).

2 There are remains such as floor coverings and pottery at Kaysanlı, a historical area not excavated by archaeologists and located near Sfard or Sardis, the capital of the Lydian Empire in the 6th century BC. Furthermore, 'Kays' represents the protagonist of Majnun Layla, based on the classic love story of Arab legend in ancient Arabia, and is the actual name of Mecnun-i Amiri, named after a small island in the Sea of Oman, ''سيق'' in Arabic. 'Anlı' means <a famous person> in Turkish. We think that Majnun may have come here if the legend is true.

Table 6. Dominant facies, facies descriptions and interpretations for the Yenipazar Formation.

Çizelge 6. *Yenipazar Formasyonu'nun baskın fasiyesleri, fasiyes tanımları ve yorumları.*

Facies	Description	Interpretation
Gms, matrix-supported gravel stones	Gravel stones with pink and yellow color silty matrix and carbonate cement, matrix-supported, moderately to poorly sorted, polymictic sub-rounded to rounded clasts, normal to reverse grading, erosive-based; dimensions: bed thickness up to 50 cm; lateral extent few tens of meters	Channel fills
Sp, pebbly sandstones	Coarse- and fine-grained sandstones with yellow and pink silty matrix and carbonate cement, matrix-supported, poorly sorted, normal to reverse graded; dimensions: bed thickness up to 1.2 m; lateral extent few tens of meters	Deposits of flash flood/ channel deposits
Sfg, fine-grained sandstones	Fine-grained sandstones, poorly sorted, bedded, laminated; dimensions: bed thickness up to 50 cm; lateral extent few tens of meters	Waning currents in channel
M, mudstones	Mudstones, laminated; dimensions: bed thickness up to 40 cm; lateral extent tens of meters	Overbank
C, lignite and bituminous coals	Coals, dark gray color, laminated; dimensions: bed thickness up to 40 cm; lateral extent less than ten meters	Overbank

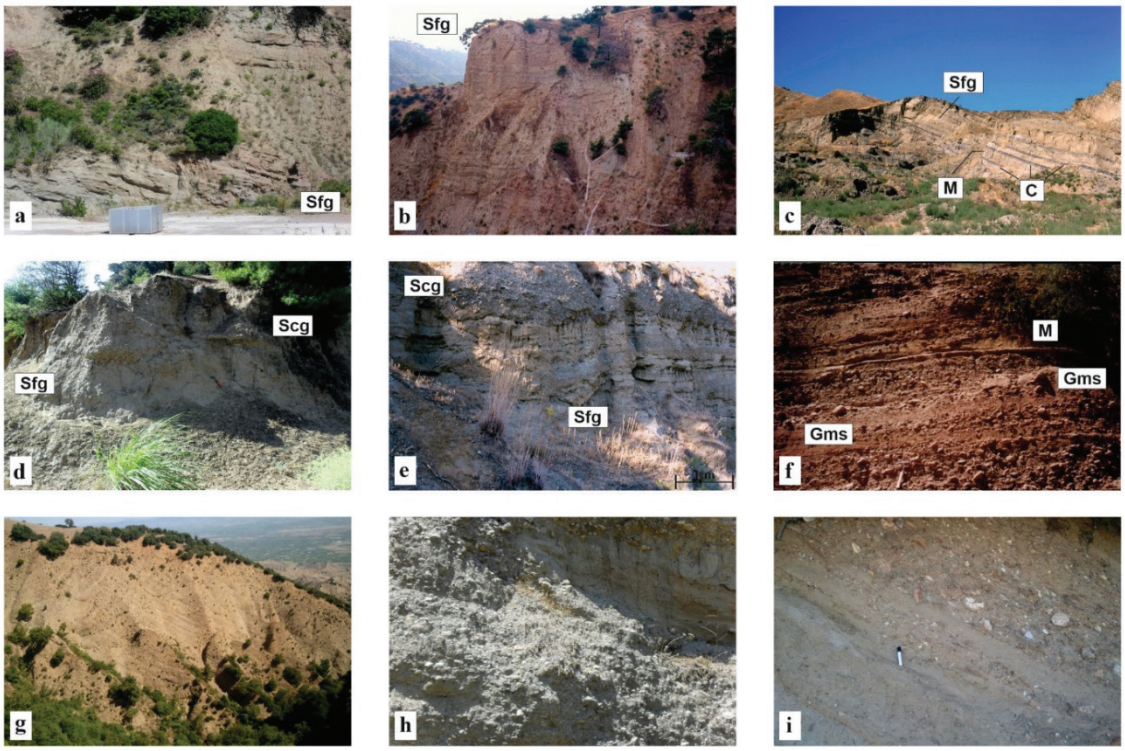

Figure 16. Outcrop views of the Upper Pliocene and the Plio-Quaternary sedimentary rocks of the Alaşehir Graben (photos taken from Şen, 2004; Ağırbaş, 2006). **(a-b)** The Yenipazar Formation contains fine-grained sandstones (facies Sfg). **(c)** The Yenipazar Formation consists mainly of fine-grained sandstones (facies Sfg) and mudstones (facies M) interbeds alternating with lignite and bituminous coal horizons (facies C). **(d-e)** The Erendalı Formation contains fine- and coarse-grained clastics (facies Sfg and Scg). **(f)** There are sub-rounded to rounded clasts (Gms), lacking cataclastic rocks of the Alaşehir detachment fault, in the Erendalı Formation. **(g)** The Asartepe Formation forms a series of sharp ridges, **(h)** and consists of angular to rounded clasts of older rocks including cataclastic rocks **(i)**.

Şekil 16. *Alaşehir Grabeni'nin Üst Pliyosen ve Pliyo-Kuvaterner tortul kayaçlarının mostra görünümleri (Şen, 2004; Ağırbaş, 2006'dan alınan fotoğraflar).* ***(a-b)*** *Yenipazar Formasyonu ince-taneli kumtaşları (Sfg fasiyesi) içerir.* ***(c)*** *Yenipazar Formasyonu esas olarak linyit ve bitümlü kömür horizonlarıyla (C fasiyesi) ardalanmalı ince-taneli*

kumtaşları (Sfg fasiyesi) ve çamurtaşları (M fasiyesi) ara katmanlarından oluşur. ***(d-e)*** *Erendalı Formasyonu ince- ve kaba-taneli kırıntılıları (Sfg ve Scg fasiyesi) içerir.* ***(f)*** *Erendalı Formasyonu'nda Alaşehir sıyrılma fayının kataklastik kayaçlarından yoksun, yarı-yuvarlak ila yuvarlaklaşmış kırıntılılar (Gms) bulunur.* ***(g)*** *Asartepe Formasyonu bir dizi keskin sırt oluşturur* ***(h)*** *ve kataklastik kayaçlar* ***(i)*** *dahil olmak üzere daha eski kayaçların köşeli ila yuvarlak parçalarından oluşur.*

Interpretation

The presence of lignite and bituminous coal horizons in the Yenipazar Formation suggests that the depositional environment of this unit is lacustrine, as suggested by some researchers (e.g., İztan and Yazman, 1990). However, the presence of sub-rounded and rounded clasts of conglomerates and laminations in the sandstone-conglomerate interbeds and pedogenic slickensides in the mudstone beds indicates that the depositional setting is a floodplain. It is noted that the sandstone-conglomerate levels in this pile are channel deposits and the peat levels are overbank deposits. This means that it is an extension of the Göbekli Formation.

Erendalı Formation

The Erendalı Formation is exposed in Erendalı Hill in the southeast of the Salihli area (Figure 3). The thickness of the Erendalı Formation is 116 m from the measured stratigraphic log in Erendalı Hill (Figure 14c), although its maximum thickness was estimated to be ~250 m based on B-B' cross-section (Figure 4; Şen, 2004). Four lithofacies are defined in the Erendalı Formation, including FA9 (floodplain facies association) (Tables 2 and 7). FA9 refers to the predominance of coarse- and fine-grained sandy beds with a minor presence of coarse-grained beds.

FA9: The floodplain facies association is composed of Gms, Sfg, Scg and M facies (Table 7; Figure 14b). The facies association is dominated by gravel stones (facies Gms) with sandy facies (Sfg and Scg) alternating with muddy beds (facies M) (Figure 8d-e). The gravel stones in FA9 consist of sub-rounded and rounded older clasts. The clasts range in size from 1 to 30 cm. The thickness of the beds ranges from 20 cm to 1 m. Coarse- and fine-grained sandstones (facies Sfg and Scg) are moderately to poorly sorted, thin- to medium-bedded. They have normal-reverse grading and laminations (Figures 14c, 16e-f).

Table 7. Dominant facies, facies descriptions and interpretations for the Erendalı Formation.
Çizelge 7. *Erendalı Formasyonu'nun baskın fasiyesleri, fasiyes tanımları ve yorumları.*

Facies	Description	Interpretation
Gms, matrix-supported gravel stones	Gravel stones with pink and yellow silty matrix and carbonate cement, matrix-supported, moderately to poorly sorted, polymictic sub-rounded to rounded clasts, normal to reverse grading, erosive base; dimensions: bed thickness up to 40 cm; lateral extent few tens of meters	Channel fills
Sfg, fine-grained sandstones	Fine-grained sandstones, poorly sorted, cross-bedded, laminated; dimensions: bed thickness up to 20 cm; lateral extent few tens of meters	Deposits of flash flood/channel deposits
Scg, coarse-grained sandstones	Coarse-grained sandstones, poorly sorted, normal and reverse graded, cross-bedded, laminated; dimensions: bed thickness up to 50 cm; lateral extent few tens of meters	Channel deposits
M, mudstones	Mudstones, laminated; dimensions: bed thickness up to 20 cm; lateral extent tens of meters	Muddy channel

Interpretation

FA9 forms coarse- and fine-grained beds representing a repetitive succession and this association is indicative of floodplain deposition. It is noticeable that the Erendalı Formation continues as successive packages and a monotonous sequence like the Göbekli and Yenipazar Formations. Therefore, the Erendalı Formation is part of the fluvial channel-fills of the Göbekli Formation in the floodplain.

Asartepe Formation

A measured stratigraphic log could not be made for the Asartepe Formation. This is because it forms sharp ridges in the study area. Its maximum thickness was estimated to be ~600 m based on A-A', C-C', D-D' and E-E' cross-sections (Figures 4 and 16g-h; Şen, 2004; Ağırbaş, 2006).

The Asartepe Formation consists of massive to poorly bedded, poorly sorted, clast-supported, yellow conglomerate with medium- to coarse-grained sandstone-siltstone beds. The conglomerate is clast-supported, with pebbles and boulders ranging from 5 mm to 40 cm in a calcareous matrix. The clasts range in size from 5 mm to 40 cm. The deposit is pebbly in the upper and lower parts (Figure 16g-h).

Interpretation

The presence of pebble imbrications, angular to rounded clasts and thin sandstone layers above the conglomerate proves that the depositional setting was a fluvial-controlled alluvial fan under the control of Plio-Quaternary normal faults instead of the ADF. This is because the size of the clasts in the detachment fault cataclastic rocks is relatively small compared to the sizes in the Miocene units (Figure 8i).

DISCUSSION

The sequences in the Alaşehir Graben consist of well-developed sedimentary rocks that extend from the Miocene to the Plio-Quaternary without any unconformities[3] (Figure 2; Emre, 1996; Şen et al., 2024). The Miocene sequence consists of three packages, including the lacustrine deposits known as the Gerentaş-Kaypaktepe Formations and the fluvial-alluvial deposits known as the Acıdere Formation, while the Plio-Quaternary sequence represents the fluvial-alluvial deposits known as the Asartepe Formation (Figure 2; Şen, 2004; Ağırbaş, 2006; Şen et al., 2024). If Gölmarmara Lake in the Salihli-Alaşehir Plain outside the study area is included, the Miocene and Plio-Quaternary sedimentary rocks in the Alaşehir Graben were deposited in similar depositional environments, including lacustrine, fluvial and alluvial-fan depocenters. They are separated from each other by floodplain deposits, which have a monotonous sequence and ages from the Upper Miocene to the Upper Pliocene (e.g., Emre, 1996; Purvis and Robertson, 2005). The floodplain deposits in the study area are represented by the Göbekli, Yenipazar and Erendalı Formations (Figures 12, 13 and 14).

The Acıdere Formation, which was deposited in fluvial and alluvial fan depocenters under the control of the ADF and its synthetic and antithetic faults, passes conformably into the Göbekli Formation (Emre, 1996; Şen et al., 2024) (Figure 2). The lower parts of the Göbekli Formation, comprising the first 140 meters, form the alluvial-fan and fluvial deposits under the control of the

3 No significant unconformity was observed in this study, although some previous studies indicated the presence of one. This may be due to local depositional variations or different structural interpretations. Some researchers claim that there are discordance planes between the Pliocene and Plio-Quaternary successions in the Alaşehir Graben (Yılmaz et al., 2000; Seyitoğlu et al., 2002; Bozkurt and Sözbilir, 2004; Öner and Dilek, 2011, 2013; Seyitoğlu and Işık, 2015). However, the Göbekli Formation is conformably covered by the Yenipazar Formation, which has a gradual transition to the Asartepe Formation (Şen et al., 2024, Figure 7b, e, page of 29).

ADF and its synthetic and antithetic faults (Figure 12). There are three reasons for this view. The shapes of the clasts in the blocky conglomerates and pebbly sandstones are angular to sub-angular (Figures 12–14 and 15d-e-f). In this part of the deposit, the size of the clasts in the lower levels is relatively small compared to the sizes in the upper levels (Figure 15e-f). There are clasts of cataclastic rocks from the ADF (Figure 15d-e). After this level, the Göbekli Formation becomes a monotonous sequence without any tectonic activity of the ADF. There are four reasons why this point of view is important. The deposit continues as successive packages (Figures 12, 13, 14a and 15a-b). There are repeated erosional base structures over fine-grained sandstone beds, and the shape of the clasts is sub-rounded and rounded in the coarse-grained clastics, and no angular clasts come from the cataclastic rocks of the ADF (Figure 15g, i). The Göbekli Formation was therefore deposited without tectonic control, except for the first 140 meters. The presence of erosional base structures on fine-grained clastics in a repetitive monotonous sequence proves that the Göbekli Formation was deposited on a floodplain after the first 140 meters. Therefore, the beds in the coarse- and fine-grained clastic intercalations of the Göbekli Formation, except for the first 140 meters, represent the channel deposits of braided streams, and the fine-grained clastics in this fill also represent overbank deposits in the floodplain depocenter.

Öner and Dilek (2011, 2013) reported that the variability in thickness of the Göbekli Formation is associated with NNE-SSW trending scissor or hinge faults, which control the deposition of the sequence in the southern margin of the Alaşehir Graben. However, there are no structural data such as planes, slickensides and grooves of scissor-hinge faults, which have an oblique-slip component, along the bottoms and slopes of NNE-SSW trending valleys (Şen, 2004; Ağırbaş, 2006; Şen and Ağırbaş, 2012; Ağırbaş and Şen, 2012; Şen et al., 2024). These faults are small reverse faults that do not cut the Göbekli-Yenipazar-Erendalı Formations, and they represent extensional structures formed by layer-parallel shortening during the Miocene (Şen et al., 2024). Furthermore, this view is contradicted by the depositional record of the Göbekli Formation (Figures 12, 13 and 14a). This is because the clasts in the Göbekli Formation are sub-rounded and rounded, except for the first 140 meters where sedimentation was controlled by the ADF and its synthetic and antithetic faults (Figure 12). Deposits thin or thicken away from channel edges depending on local floodplain morphology, and floodplain deposits are not observed with the same thickness everywhere due to differences in topography between channel-bars and -fills in this depocenter (Willis and Behrensmeyer, 1994). Bed splays exhibit either upward-coarsening or upward-fining fills (Smith and Perez-Arlucea, 1994). Thus, the change in thickness of the Göbekli Formation depends on the difference in topography between the channel-bars and -fills in the floodplain (Figure 12–14a).

The Yenipazar Formation is defined as a lacustrine sequence based on fine-grained clastic sedimentary rocks intercalated with lignite and bituminous coal horizons and medium- to thick-bedded organic clay layers and pedogenic slickensides in the mudstone beds (e.g., İztan and Yazman, 1990; Yılmaz et al., 2000; Purvis and Robertson, 2005; Öner and Dilek, 2011, 2013). However, tabular deposits of clay, silt and organic particulates fill flood-basin depressions (Figure 14b). Water levels fluctuated seasonally and smectitic clays are present and pedogenic slickensides are abundant in the depocenter. In contrast, perennial saturation and low levels of clastic input led to widespread peat and coal formation (Flores, 1981). Therefore, these depositional environments are often erroneously defined as lacustrine depocenters (Farrell, 1987; Gerard, 2003). Floodplain deposits provide

a monotonous sequence and are depositional settings that occur during a period of tectonic quiescence (e.g., Kraus, 1999). Thus, the Yenipazar Formation overlying the Göbekli Formation is part of the floodplain deposits (Figure 14b). This is because the fill is as monotonous as the Göbekli Formation (Figures 12, 13 and 14b). If the Yenipazar Formation were a lake sequence, it should have the lithological characteristics of the Gerentaş-Kaypaktepe Formations, which are Early-Middle Miocene sequences in the Alaşehir Graben as shown in Figure 6a-b. Additionally, the Yenipazar Formation is part of the overbank deposits in the Göbekli Formation and the Erendalı Formation forms the channel-fills of braided streams in the Yenipazar Formation based on their sedimentological features (Figure 14b-c).

The Miocene to Late Pliocene sequence in the Alaşehir Graben was deposited during activity on the ADF, according to Seyitoğlu et al. (2002). But the sedimentological record of the deposits shows that the ADF and its synthetic and antithetic faults became inactive shortly after the deposition of the Göbekli Formation (Figure 12–14). Two important structural data sets supporting this event are available in the Alaşehir Graben. (a) The synthetic and antithetic faults belonging to the ADF do not cut the floodplain deposits consisting of the Göbekli, Yenipazar and Erendalı Formations (Figures 3 and 4; Şen et al., 2024). Experimental studies showed that when normal faulting occurs deep in the earth, traces of faulting, such as fault plane or surface ruptures, are not visible on the surface (Oertel, 1965). Therefore, traces of these faults may not be observed in these formations. However, if there was faulting at depth in the earth during the time of their formation, then materials from sudden debris flows from high morphology areas on the surface into the basin should be present in these units, and a scatter in the geometry of the clasts in these materials is expected. However, both the size and geometry of the clasts are uniform across the units (Table 5, 6, 7). (b) Small-scale reverse faults cutting the Lower-Upper Miocene fills in the papers of Öner and Dilek (2011, 2013) represent extensional structures formed by layer-parallel shortening and they are not observed in the post-Miocene fills (Şen et al., 2024). This means that these structures were formed in the early to late Miocene, which corresponds to the period when the ADF was active.

In summary, the most recent period of tectonic activity on the ADF and its synthetic and antithetic faults was in the Late Miocene (c. 6-5.5 Ma), as stated by Lips et al. (2001) (Şen et al., 2024). This corresponds to recent movement of the detachment faults in the Rhodope, Kazdağ, Çataldağ, Uludağ, Menderes and Cycladic metamorphic core complexes (c. 12-6 Ma; U-Th/He zircon and apatite ages, Thomson and Ring, 2006; Okay et al., 2008; Cavazza et al., 2009; Kounov et al., 2015; Wölfler et al., 2017; Heineke et al., 2019; Altunkaynak et al., 2021; Lamont et al., 2023). The recent movement of the detachment faults controlling the core complexes becomes progressively younger from north to south (Figure 1a). The reason for this is probably that the Arabian continent collided with Anatolia in the latest Middle-earliest Late Miocene (Serravallian-Tortonian transition), and the Anatolian Block escaped westward along a larger displacement zone called the "North Proto-Anatolian Transform" by Dewey and Şengör (1979). When Western Anatolia is divided into northern and southern sectors (Figure 1a), this effect is seen immediately in the northern sector (c. 12-10 Ma), whereas it occurs over time in the southern sector (c. 6-5.5 Ma). In other words, the effect of the westward escape of the Anatolian Block lasted ~ 6-4 million years from the northern sector to the southern sector in Western Anatolia. It is clear from the literature that volcanism ceased during this period, as did tectonism in the region (see the papers of Helvacı et al., 2009, page of 183; Ersoy et al., 2012, page of 380) (Figure 1b). The change in the paleo-position of the subducting African oceanic lithosphere may have

been responsible for the cessation of tectonism and volcanism during the Late Miocene to Late Pliocene.

There are literature reports that the most recent movement of the ADF was in the Pliocene. The first of these reports is Early Pliocene (c. 4.5 ± 1.0 Ma; Th-Pb monazite, Catlos and Çemen, 2005). However, it could be either Late Miocene or Late Pliocene due to the high margin of error. According to the stratigraphic logs measured in this paper, the Upper Miocene-Lower Pliocene Göbekli Formation shows that the unit was deposited without any tectonic activity except for the first 140 meters (Figure 12-13-14a). This is evidenced by the fact that the clasts in the unit after the first 140 meters are round and semi-round (Figure 12-13-14a). In the Mississippi Basin, which is shaped by active tectonics (Cox et al., 2000), current clasts are round and sub-rounded. However, these clasts have acquired this geometry by being transported for approximately 3750 km (Bentley et al., 2016). The distance between the Göbekli Formation and the ADF in the Alaşehir Graben varies between 500 meters and 1 km (Figure 3). This means that the clasts of the Göbekli Formation were not deposited after transport over long distances. Thus, this radiometric age, with a high margin of error, probably represents the Late Miocene. This is because it coincides with the age of Lips et al. (2001), which is equivalent to with the recent frictional time of the ADF, and explains why the geometry of the clasts in the first 140 meters of the Göbekli Formation is angular and sub-angular. Besides, the Pliocene ages (4 Ma, K-Ar whole rock) obtained by Hetzel et al. (2013) are not supported in the data set (3.5-2.0 Ma, apatite and zircon fission track) of Buscher et al. (2013) (see Seyitoğlu et al. (2014) for a detailed review; Table 1, pages of 485-486). In other words, whole-rock ages obtained with the K-Ar dating method are not reliable for use today. Buscher et al. (2013) do not have 4 Ma data sets.

Plio-Quaternary thermal ages (c. 3.10-1.75 Ma, apatite fission track, Gessner et al., 2001; c. 3.50-0.80 Ma, apatite fission track and c. 3.5-2.0 Ma, zircon fission track, Buscher et al., 2013) indicate that the footwall and hanging wall of the ADF were exhumed under the control of Plio-Quaternary high-angle normal faults (Şen et al., 2024). Depositional records in the Asartepe Formation support the Plio-Quaternary thermal ages, corresponding to angular to rounded clasts, including high-grade metamorphic rocks of the Menderes Massif and cataclastic rocks of the ADF.

Overall, Miocene sedimentation took place under the control of the ADF and its synthetic and antithetic faults, and the Plio-Quaternary high-angle normal faults controlled the Plio-Quaternary sedimentation. They are separated from each other by floodplain deposits, which represent a period of tectonic quiescence during the late Miocene to late Pliocene. This suggests a two-stage rifting model, without contraction phases, during the Late Miocene to Late Pliocene (Bozkurt and Sözbilir, 2004; Şen et al., 2024).

CONCLUSION

In this paper, we presented measured stratigraphic logs of Miocene-Pliocene sedimentary rocks from the southern margin of the Alaşehir Graben from studies by Şen (2004) and Ağırbaş (2006), which allow us to explain the termination of the tectonic activity of the Alaşehir Detachment Fault.

The sedimentary rocks in the Alaşehir Graben are divided into three sequences, including the Lower-Upper Miocene (Gerentaş, Kaypaktepe and Acıdere Formations), the Upper Miocene-Upper Pliocene (Göbekli, Yenipazar and Erendalı Formations) and the Plio-Quaternary successions (Asartepe Formation). The Miocene and Plio-Quaternary successions were deposited in similar depocenters, including lacustrine, fluvial and alluvial-fan environments. They are separated

by floodplain deposits, which are monotonous in sequence and range in age from Upper Miocene to Upper Pliocene. The floodplain deposits on the southern margin of the Alaşehir Graben include the Göbekli, Yenipazar and Erendalı Formations. The floodplain deposits are a monotonous sequence that repeats itself and is not tectonically mobile after the first 140 meters from the stratigraphic bottom based on sub-rounded to rounded clasts of cataclastic rocks belonging to the Alaşehir detachment fault. They represent a period of tectonic quiescence during the Late Miocene to Late Pliocene, thus indicating the termination of the tectonic activity on the Alaşehir Detachment Fault during the Late Miocene.

GENİŞLETİLMİŞ ÖZET

Alaşehir Grabeni'nin güney kenarı, aynı gerilmeli rejim içerisindeki sünek ve kırılgan kataklastik kayaçlar içeren Alaşehir Sıyrılma Fayı ile sınırlanmıştır (Işık vd., 2003; Şen vd., 2024). Bu sıyrılma fayı, Turgutlu'dan Alaşehir'e kadar yaklaşık 150 km boyunca yüzeylenmiş (Emre, 1996; Işık vd., 2003) ve kuzeye düşük bir açı (10^0-30^0) ile eğimli olan yüzeydir (Çemen vd., 2005; Şen vd., 2024). Alaşehir Sıyrılma Fayının tektonik aktivitesinin sonlanmasını yorumlayan iki temel görüş vardır. Birincisi, fayın son hareketinin, Pliyo-Kuvaterner yüksek açılı normal faylar tarafından kesilmiş olması gerçeğine dayanarak Geç Miyosen'de sona erdiğidir (Bozkurt ve Sözbilir, 2004; Şen vd., 2024). Diğer görüş ise, Alaşehir sıyrılma fayına ait kataklastik kayaçlardan elde edilen yüzeylenme yaşlarına dayanarak tektonik aktivitesinin Pliyo-Kuvaterner'e kadar devam ettiğidir (Seyitoğlu vd., 2002; Seyitoğlu ve Işık, 2015).

Bu makale, bu tartışmaya katkıda bulunmak için Salihli ve Alaşehir bölgelerindeki Alaşehir Sıyrılma Fayının tavan bloğundaki Neojen tortul kayalarının ölçülü stratigrafik kesitlerini Alaşehir Sıyrılma Fayı' na ait kataklastik kayaçlarının ve Menderes Masifi' nin yüksek dereceli metamorfik kayaçlarına ait çakıl ve blokların küreselliği esasına göre rapor edilmektedir. Sedimantolojik kayıtlar, Alaşehir Grabeni'nin güney kenarında 2003 yaz döneminde üç ay süren Şen (2004) ve Ağırbaş (2006) tarafından yapılan iki bitirme tezine aittir.

Yapılan ölçülü stratigrafik kesitlere göre, Alaşehir Grabeni'nin güney kenarının sedimantasyon evrimi Erken-Geç Miyosen, Geç Miyosen-Geç Pliyosen ve Pliyo-Kuvaterner dönemi olarak ayrılır. Erken-Geç Miyosen ve Pliyo-Kuvaterner dönemleri göl, akarsu ve alüvyal yelpaze ortamları olmak üzere benzer sedimantasyon ortamları ile temsil edilir. Bu iki dönem taşkın yatağı sedimantasyon ortamını temsil eden Geç Miyosen-Geç Pliyosen zamanı ile ayrılmaktadır. Taşkın yatağı çökelleri, Alaşehir Sıyrılma Fayı' na ait kataklastik kayaçların yarı-yuvarlak ve yuvarlak kırıntılarına dayanarak stratigrafik tabandan itibaren ilk 140 metreden sonra tektonik olarak hareketli olmayan ve kendini tekrarlayan monoton bir istiftir. Bunlar, Geç Miyosen-Geç Pliyosen zamanında oluşan tektonik sessizlik dönemini temsil eder ve Alaşehir Sıyrılma Fayı' ndaki tektonik aktivitenin Geç Miyosen döneminde sonlandığını gösterir.

ACKNOWLEDGEMENTS

This paper is part of two BSc theses (Şen, 2004; Ağırbaş, 2006). The geologist Hakan Ağırbaş, who has left the earth sciences, gave his permission to publish his theses in this study with other researchers. The corresponding author would like to thank T. Ustaömer of İstanbul University for his thoughtful review and constructive comments during the preparation of the thesis. He would also like to thank the people of the villages of Yenipazar and Alkan in Salihli and Alaşehir for their help during the fieldwork. We thank the Editor-in-Chief, E. Yiğitbaş, and five anonymous reviewers for their thoughtful review and constructive criticism of our manuscript.

DECLARATIONS

Conflict of interest: The authors declare no conflict of interest.

ORCID

Fatih Şen https://orcid.org/0000-0002-9227-6324
Serdal Karaağaç https://orcid.org/0000-0002-2458-3269

REFERENCES

Ağırbaş, H. (2006). *Alkan köyü (Alaşehir) ve yakın çevresinde Gediz grabeni' nin stratigrafisi ve yapısal özellikleri* [B.Sc. thesis]. İstanbul, İstanbul University, (in Turkish), 115 pp.

Ağırbaş H. & Şen, F. (2012). Neogene-Quaternary stratigraphy and tectonics of Alaşehir graben, Western Anatolia. *International Earth Science Colloquium on the Aegean Region, Proceedings* (pp:38), 1-5 October 2012, İzmir, Turkey.

Akbayram, K., Şengör, A.M.C. & Özcan, E. (2016). The evolution of the Intra-Pontide suture: implications of the discovery of late Cretaceous–early Tertiary melanges. *Geological Society of America Special Papers, 525*, SPE525-18.

Altunkaynak, Ş., Ünal, A., Sunal, G., Kamacı, Ö. & Dunkl, I. (2021). Miocene uplift and exhumation history of northwestern Anatolia (Turkey): Implications from apatite (U-Th)/He thermochronology of syn-extensional plutons. *Journal of Asian Earth Sciences, 213*, Article104770. https://doi.org/10.1016/j.jseaes.2021.104770

Arpat, E. & Bingöl, E. (1969). The rift system of western Turkey: Thoughts on its development. *Bulletin of the Mineral Research and Exploration Institute, 75*, 1-9.

Baes, M., Govers, R. & Wortel, R. (2011). Subduction initiation along the inherited weakness zone at the edge of a slab: Insights from numerical models. *Geophysical Journal International, 184*(3), 991–1008. https://doi.org/10.1111/j.1365-246X.2010.04896.x

Bentley, S. J., Blum, M. D., Maloney, J., Pond, L. & Paulsell, R. (2016). The Mississippi River source-to-sink system: Perspectives on tectonic, climatic, and anthropogenic influences, Miocene to Anthropocene. *Earth-Science Reviews, 153*, 139–174. https://doi.org/10.1016/j.earscirev.2015.11.001

Biryol, C. B., Beck, S. L., Zandt, G. & Özacar, A. A. (2011). Segmented African lithosphere beneath the Anatolian region inferred from teleseismic P-wave tomography. *Geophysical Journal International, 184*, 1037–1057. https://doi.org/10.1111/j.1365-246X.2010.04910.x

Bozkurt, E. (2000). Timing of extension on the Büyük Menderes Graben, western Turkey, and its tectonic implications. In E. Bozkurt, E., Winchester, J.A., Piper, J.D.A (Eds.), *Tectonics and Magmatism in Turkey and the Surrounding Area, Geological Society, London, Special Publications 173*, 385-403.

Bozkurt, E. (2001). Neotectonics of Turkey-a synthesis. *Geodinamica Acta 14*, 3-30. https://doi.org/10.1016/S0985-3111(01)01066-X

Bozkurt, E. (2003). Origin of NE-trending basins in western Turkey. *Geodinamica Acta, 14*, 61–81.

Bozkurt, E. & Park, R. G. (1994). Southern Menderes Massif: an incipient metamorphic core complex in western Anatolia, Turkey. *Journal of the Geological Society, London, 151*, 213–216.

Bozkurt, E. & Sözbilir, H. (2004). Tectonic evolution of the Gediz Graben: field evidence for an episodic, two extension in western Turkey. *Geological Magazine 141*, 63–79. https://doi.org/10.1017/S0016756803008379

Bozkurt, E. & Rojay, B. (2005). Episodic, two-stage Neogene extension and short-term intervening compression in Western Turkey: field evidence from the Kiraz Basin and Bozdağ Horst. *Geodinamica Acta 18*, 299–316.

Bølviken, B., Bogen, J., Jartun, M., Langedal, M., Ottesen, R. T. & Volden, T. (2004). Overbank sediments: a natural bed blending sampling medium for large—scale geochemical mapping. *Chemometrics and Intelligent Laboratory Systems 74* (2004), 183 – 199.

Buscher, J.T., Hampel, A., Hetzel, R., Dunkl, I., Glotzbach, C., Struffert, A., Akal, C. & Ratz, M. (2013). Quantifying rates of detachment faulting and erosion in the central Menderes massif

(western Turkey) by thermochronology and cosmogenic 10Be. *Journal of Geological Society London, 170*, 669-683. https://doi.org/10.1144/jgs2012-132

Candan, O., Dora, O., Oberhänsli, R., Çetinkaplan, M., Partzch, J., Warkus, F. & Dürr, S. (2001). Pan-African high-pressure metamorphism in the Precambrian basement of the Menderes Massif, western Anatolia, Turkey. *International Journal of Earth Sciences, 89*, 793–811. https://doi.org/10.1007/s005310000097

Catlos, E. J. & Çemen, İ. (2005). Monazite ages and rapid exhumation of the Menderes Massif, western Turkey. *International Journal of Earth Sciences, 94*, 204 – 217. https://doi.org/10.1007/s00531-005-0470-7

Catlos, E. J., Baker, C., Sorensen, S. S., Çemen, İ. & Hançer, M. (2010). Geochemistry, geochronology and cathodoluminescence imagery of the Salihli and Turgutlu granites (Central Menderes Massif, western Turkey): Implications for Aegean tectonics. *Tectonophysics, 488*(1-4), 110-130. https://doi.org/10.1016/j.tecto.2009.06.001

Cavazza, W., Okay, A. I. & Zattin, M. (2009). Rapid early middle Miocene exhumation of the Kazdağ Massif (western Anatolia): *International Journal of Earth Sciences, 98,* 1935–1947. https://doi.org/10.1007/s00531-008-0353-9

Cohen, H. A., Dart, C. J., Akyüz, H. S. & Barka, A. (1995). Syn-rift sedimentation and structural development of the Gediz and Büyük Menderes Graben, western Turkey. *Journal of the Geological Society, 152*, 629–638. https://doi.org/10.1144/gsjgs.152.4.0629

Cox, R. T., van Arsdale, R. B., Harris, J. B., Forman, S. L., Beard, W. & Galluzzi, J., (2000). Quaternary faulting in the southern Mississippi embayment and implications for tectonics and seismicity in an intraplate setting. *GSA Bulletin 112*, 1724–1735. https://doi.org/10.1130/0016-7606(2000)112%3C1724:QFITSM%3E2.0.CO;2

Çemen, İ., Göncüoğlu, M. C. & Dirik, K. (1999). Structural evolution of the Tuzgölü basin in Central Anatolia, Turkey. *Journal of Geology, 107*, 693–706, https://doi.org/10.1086/314379.

Çemen, İ., Tekeli, O., Seyitoğlu, G. & Işık, V. (2005). Are turtleback fault surfaces common tectono-morphologic features of highly extended terranes?. *Earth Science Reviews, 73*, 139–148, https://doi.org/10.1016/j.earscirev.2005.07.001

Çemen, İ., Catlos, E. J., Göğüş, O. & Özerdem, C. (2006). Postcollisional extensional tectonics and exhumation of the Menderes massif in the Western Anatolia extended terrane. In Dilek, Y. & Pavlides, S. (Eds.) *Postcollisional tectonics and magmatism in the Mediterranean region and Asia. Geological Society of America Special Paper, 409*, 353–379. https://doi.org/10.1130/2006.2409(18)

Çiftçi, N. B. & Bozkurt, E. (2008). Folding of the Gediz Graben fill, SW Turkey: extensional and/or contractional origin?. *Geodinamica Acta, 21*, 145-167. https://doi.org/10.3166/ga.21.145-167

Çiftçi, N. B. & Bozkurt, E. (2009). Evolution of the Miocene sedimentary fill of the Gediz Graben, SW Turkey. *Sedimentary Geology, 216*(3-4), 49-79. https://doi.org/10.1016/j.sedgeo.2009.01.004

Çiftçi, N. B. & Bozkurt, E. (2010). Structural evolution of the Gediz Graben, SW Turkey temporal and spatial variation of the graben basin. *Basin Research, 22*, 846-873. https://doi.org/10.1111/j.1365-2117.2009.00438.x

Dewey, J. F. & Şengör, A. M. C. (1979). Aegean and surrounding regions: complex multiplate and continuous tectonics in a convergent zone. *Geological Society of America Bulletin, 90*, 84–92.

Dora, O.Ö., Candan, O., Kaya, O., Koralay, E. & Dürr, S. (2001). Revision of "Leptite-gneisses" in the Menderes Massif: a supracrustal metasedimentary origin. *International Journal of Earth Sciences, 89*, 836-851. https://doi.org/10.1007/s005310000102

Dunbar, C. O. & Rodgers, J. (1957). *Principles of Stratigraphy*. John Wiley and Sons (Chapman and Hall), London, 1957.

Ediger, V., Batı, Z. & Yazman, M. (1996). Palynology of possible hydrocarbon source rocks of the Alaşehir- Turgutlu area in the Gediz graben (western Anatolia). *Turkish Association of Petroleum Geologists Bulletin, 8*, 94-112.

Edwards, M. A. & Grasemann, B. (2009). Mediterranean snapshots of accelerated slab retreat: subduction instability in stalled continental collision. In van Hinsbergen D. J. J., Edwards M. A. & Govers,

R. (Eds.), *Collision and collapse at the Africa-Arabia-Eurasia subduction zone. The Geological Society, London, Special Publication, 311*, 155–192

Elitez, İ., Yaltırak, C. & Sunal, G. (2018). A new chronostratigraphy (^{40}Ar-^{39}Ar and U-Pb dating) for the middle section of the Burdur-Fethiye Shear Zone, SW Turkey (eastern Mediterranean). *Turkish Journal of Earth Sciences, 27*(5), Article 4. https://doi.org/10.3906/yer-1803-14

Elmas, A., Koralay, E., Duru, O. & Schmidt, A. (2016). Geochronology, geochemistry, and tectonic setting of the Oligocene magmatic rocks (Marmaros Magmatic Assemblage) in Gökçeada Island, northwest Turkey. *Journal International Geology Review, 59*(4), 420-447. https://doi.org/10.1080/00206814.2016.1227941

Emre, T. (1996). Geology and tectonics of Gediz Graben. *Turkish Journal of Earth Sciences, 5*, 171–185.

Emre, T. & Sözbilir, H. (2007). Tectonic evolution of the Kiraz Basin, Küçük Menderes Graben: evidence for compression/uplift-related basin formation overprinted by extensional tectonics in West Anatolia. *Turkish Journal of Earth Sciences 16*, 441–470.

Erdoğan, B. & Güngör, T. (2004). The problem of the core-cover boundary of the Menderes massif and an emplacement mechanism for regionally extensive gneissic granites, western Anatolia (Turkey). *Turkish Journal of Earth Sciences 13*(1), 15-36. https://journals.tubitak.gov.tr/earth/vol13/iss1/2

Ersoy, Y. E., Helvacı, C. & Palmer, M. R. (2012). Petrogenesis of the Neogene volcanic units in the NE–SW-trending basins in western Anatolia, Turkey. *Contributions to Mineralogy and Petrology, 163*, 379–401. https://doi.org/10.1007/s00410-011-0679-3

Espurt, N., Hippolyte, J. C., Kaymakçı, N. & Sangu, E. (2014). Lithospheric structural control on inversion of the southern margin of the Black Sea Basin, Central Pontides, Turkey. *Lithosphere, 6*(1), 26-34. https://doi.org/10.1130/L316.1

Eyidoğan, H. & Jackson, J. (1985). A seismological study of normal faulting in the Demirci, Alaşehir and Gediz earthquakes of 1969–70 in western Turkey: Implication for the nature and geometry of deformation in the continental crust. *Geophysical Journal of the Royal Astronomical Society, 81*, 569–607.

Faccenna, C., Jolivet, L., Piromallo, C. & Morelli, A. (2003). Subduction and the depth of convection of the Mediterranean mantle. *Journal of Geophysical Research. 108*(B2), 2099. http://dx.doi.org/10.1029/2001JB001690 .

Faccenna, C., Bellier, O., Martinod, J., Piromallo, C. & Regard, V. (2006). Slab detachment beneath eastern Anatolia: a possible cause for the formation of the North Anatolian Fault. *Earth and Planetary Science Letters, 242*(1-2), 85–97. https://doi.org/10.1016/j.epsl.2005.11.046

Faccenna, C., Becker, T.W., Jolivet, L. & Keskin, M. (2013). Mantle convection in the middle East: reconciling Afar upwelling, Arabia indentation and Aegean trench rollback. *Earth and Planetary Science Letters, 375*, 254–269. https://doi.org/10.1016/j.epsl.2013.05.043

Farrell, K. M. (1987). Sedimentology and facies architecture of overbank deposits of Mississippi River, False River region, Louisiana. In Ethridge F. G, Flores R. M. & Harvey M. D. (Eds.), *Recent developments in fluvial sedimentology, Soc Econ Paleontol Mineral Spec Publ, 39*, 111-120. https://doi.org/10.2110/pec.87.39.0111

Fisk, H. N. (1947). *Fine-grained alluvial deposits and their effects on Mississippi River activity*. Waterways Experiment Station (U.S.), and United States, Mississippi River Commission, Vicksburg, Mississippi, 82 p.

Flores, R. M. (1981). Coal deposition in fluvial paleoenvironments of the Paleocene Tongue River Member of the Fort Union Formation, Powder River area, Powder River Basin, Wyoming and Montana. In F.G. Ethridge & R.M. Flores (Eds.), *Recent and Ancient Nonmarine Depositional Environments--Models for Exploration. Soc. Econ. Paleontol. Mineral. Spec. Publ., 31*, 169-190.

Gans, C. R., Beck, S. L., Zandt, G., Biryol, C. B. & Özacar, A. A. (2009). Detecting the limit of slab break-off in central Turkey: new high resolution Pn tomography results. *Geophysical Journal International, 179*(3), 1566–1577. https://doi.org/10.1111/j.1365-246X.2009.04389.x

Gerard, V. M. (2003). *Encyclopedia of sediments and sedimentary rocks*. Cornwall, Kluwer Academic Publishers.

Gessner, K. (2000). *Eocene Nappe Tectonics and Late-Alpine Extension in the Central Anatolide Belt, Western Turkey-Structure, Kinematics and Deformation History* [Ph.D thesis]. Johannes Gutenberg University Earth Sciences Department, Mainz, Germany.

Gessner, K., Ring, U., Johnson, C., Hetzel, R., Passchier, C. W. & Güngör, T. (2001). An active bivergent rolling hinge detachment system: Central Menderes metamorphic core complex in western Turkey. *Geology 29*, 611-614. https://doi.org/10.1130/0091-7613(2001)029<0611:AABRHD>2.0.CO;2

Gessner, K., Gallardo, L.A., Markwitz, V., Ring, U. & Thomson, S.T. (2013). What caused the denudation of the Menderes massif: review of crustal evolution, lithosphere structure, and dynamic topography in southwest Turkey. *Gondwana Research, 24*(1), 243–274. http://dx.doi.org/10.1016/j.gr.2013.1001.1005

Glodny, J. & Hetzel, R. (2007). Precise U–Pb ages of syn-extensional Miocene intrusions in the central Menderes Massif, western Turkey. *Geological Magazine 144*, 235-246. https://doi.org/10.1017/S0016756806003025

Govers, R. & Wortel, M. J. R. (2005). Lithosphere tearing at STEP faults: Response to edges of subduction zones. *Earth and Planetary Science Letters, 236*(1–2), 505–523. https://doi.org/10.1016/j.epsl.2005.03.022

Gürer, A., Gürer, Ö.F., Pinçe, A. & Ilkisik, O.M. (2001). Conductivity structure along the Gediz graben, west Anatolia, Turkey: Tectonic implications: *International Geology Review, 43*, 1129-1144. https://doi.org/10.1080/00206810109465065

Heineke, C., Hetzel, R., Nilius, N.P., Zwingmann, H., Todd, A., Mulch, A., Wölfler, A., Glotzbach, C., Akal, C., Dunkl, I. & Raven, M. (2019). Detachment faulting in a bivergent core complex constrained by fault gouge dating and low-temperature thermochronology. *Journal of Structural Geology, 127*, Article 103865. https://doi.org/10.1016/j.jsg.2019.103865

Helvacı, C., Ersoy, E.Y., Sözbilir, H., Erkül, F., Sümer, Ö. & Uzel, B. (2009). Geochemistry and $^{40}Ar/^{39}Ar$ geochronology of Miocene volcanic rocks from the Karaburun Peninsula: implications for amphibole-bearing lithospheric mantle source, western Anatolia. *Journal of Volcanology and Geothermal Research, 185*(3), 181–202. https://doi.org/10.1016/j.jvolgeores.2009.05.016

Hetzel, R., Passchier, C. W., Ring, U. & Dora, Ö. O. (1995). Bivergent extension in orogenic belts: the Menderes massif (southwestern Turkey). *Geology 23,* 455–458.

Hetzel, R., Zwigmann, H., Mulch, A., Gessner, K., Akal, C., Hampel, A., Güngör, T., Petschick, R., Mikes, T. & Wedin, F (2013). Spatiotemporal evolution of brittle normal faulting and fluid infiltration in detachment fault systems: a case study from Menderes massif, western Turkey. *Tectonics, 32*(3) 364-376. https://doi.org/10.1002/tect.20031

Hippolyte, J.C., Müller, C., Kaymakçı, N. &Sangu, E. (2010). Dating of the Black Sea Basin: new nannoplankton ages from its inverted margin in the Central Pontides (Turkey). In Stephenson, R.A., Kaymakçı, N., Sosson, M., Starostenko, V., Bergerat, F. (Eds.), *Sedimentary Basin Tectonics from the Black Sea and Caucasus to the Arabian Platform. London, UK: Geological Society London Special Publications*, 113-136.

Işık, V., Seyitoğlu, G. & Çemen, İ. (2003). Ductile-brittle transition along the Alaşehir detachment fault and its structural relationship with the Simav detachment fault, Menderes Massif, western Turkey. *Tectonophysics 374*, 1-18. https://doi.org/10.1016/S0040-1951(03)00275-0

İztan, H. & Yazman, M. (1990). Geology and hydrocarbon potential of the Alaşehir (Manisa) area, western Turkey. In Savaşçın, M. Y. & Eronat, A. H. (Eds.), Proceedings Internatioanl Earth Sciences Congress Aegean Region 1990, Izmir, pp. 327– 333.

Jackson, J. A. & McKenzie, D. P. (1988). The relationship between plate motions and seismic tensors, and the rate of active deformation in the Mediterranean and Middle East. *Geophysical Journal International, 93*, 45-73. https://doi.org/10.1111/j.1365-246X.1988.tb01387.x

Jolivet, L. & Patriat, M. (1999). Ductile extension and the formation of the Aegean Sea. In Durand, B., Jolivet, L., Seranne, M. (Eds.), *The Mediterranean Basins: Tertiary Extension Within the Alpine Orogen. Geological Society, London, Special Publications, 156*, 356–427.

Jolivet, L. & Faccenna, C. (2000). Mediterranean extension and the Africa–Eurasia collision. *Tectonics, 19*, 1095–1106. https://doi.org/10.1029/2000TC900018 .

Jolivet, L. & Brun, J. P. (2010). Cenozoic Geodynamic Evolution of the Aegean. *International Journal of Earth Sciences, 99*(1), 109–138. https://doi.org/10.1007/s00531-008-0366-4

Jolivet, L., Faccenna, C., Huet, B., Labrousse, L., Le Pourhiet, L., Lacombe, O., Lecomte, E., Burov, E., Denele, Y., Brun, J.P., Philippon, M., Paul, A., Salaun, G., Karabulut, H., Piromallo, C., Monie, P., Gueydan, F., Okay, A.I., Oberhansli, R., Pourteau, A., Augier, R., Gadenne, L. & Driussi, O. (2013). Aegean tectonics: strain localization, slab tearing and trench retreat. *Tectonophysics, 597–598*, 1–33. https://doi.org/10.1016/j.tecto.2012.06.011

Kissel, C. & Laj, C. (1988). Tertiary geodynamical evolution of the Aegean arc: a palaeomagnetic reconstruction. *Tectonophysics, 146*, 183–201.

Koçyiğit, A. &Yusufoğlu, H., Bozkurt, E. (1999). Evidence from the Gediz Graben for episodic two-stage extension in western Turkey. *Journal of the Geological Society 156*, 605-616. https://doi.org/10.1144/gsjgs.156.3.0605

Konak, N. (2002). *Geological map of Turkey in 1/500,000 scale. İzmir Area Map* (Şenel, M. (Ed.). General Directorate of Mineral Research and Exploration, Publication of Mineral Research and Exploration Directorate of Turkey.

Kounov, A., Wüthrich, E., Seward, D., Burg, J. P. & Stockli, D. (2015). Low-temperature constraints on the Cenozoic thermal evolution of the Southern Rhodope Core Complex (Northern Greece). *International Journal Earth Sciences, 104*, Article 1337e1352. https://doi.org/10.1007/s00531-015-1158-2

Kraus, M. J. (1999). Paleosols in clastic sedimentary rocks: their geologic applications. *Earth Science Reviews, 47*, 41-70.

Lamont, T. N., Smye, A. J., Roberts, N. M. W., Searle, M. P., Waters, D. J. & White, R. W. (2023). Constraints on the thermal evolution of metamorphic core complexes from the timing of high-pressure metamorphism on Naxos, Greece. *Geological Society of America Bulletin, 135*(11–12), 2767–2796. https://doi.org/10.1130/B36332.1

Le Pichon, X. & Angelier, J. (1979). The Hellenic arc and trench system: a key to the neotectonic evolution of the eastern Mediterranean area. *Tectonophysics, 60*, 1–42.

Le Pichon, X. & Angelier, J. (1981). The Aegean Sea. *Philosophical Transactions of Royal Society, London, Seri A 300*, 357–372.

Lips, A. L. W., Cassard, D., Sözbilir, H., Yılmaz, Y. & Wijbrans, J. R. (2001). Multistage exhumation of the Menderes Massif, western Anatolia (Turkey). *International Journal of Earth Sciences, 89*, 781-792.

Mack, G. H., Leeder, M. R. & Salyards, S. L. (2002). Temporal and spatial variability of alluvial-fan and axial-fluvial sedimentation in the Plio-Pleistocene Palomas half graben, southern Rio Grande rift, New Mexico, USA. In Renault, R. W. & Ashley, G. M. (Eds.), *Sedimentation in Continental Rifts. SEPM Special Publications, 73*, 165–177.

McKenzie, D. (1978). Active tectonics of the Alpine-Himalayan belt: the Aegean Sea and surrounding regions. *Geophysical Journal of Astronomical Society, 55*, 217–254.

Menant, A., Sternai, P., Jolivet, L., Guillou-Frottier, L. & Gerya, T. (2016). 3D numerical modeling of mantle flow, crustal dynamics and magma genesis associated with slab roll-back and tearing: The eastern Mediterranean case. *Earth and Planetary Science Letters, 442*, 93-107. https://doi.org/10.1016/j.epsl.2016.03.002

Mercier, J. L. (1981). Extensional-compressional tectonics associated with the Aegean arc: comparison with the Andean Cordillera of south Peru–north Bolivia. *Philosophical Transactions of Royal Society, London, Seri A 300*, 337–355.

Meulenkamp, J. E., Wortel, W. J. R., Van Wamel, W. A., Spakman, W. & Hoogerduyn-Strating, E. (1988). On the Hellenic subduction zone and geodynamic evolution of Crete in the late Middle Miocene. *Tectonophysics, 146*, 203–215.

Meulenkamp, J. E., Van Der Zwaan, G. J. & Van Wamel, W. A. (1994). On Late Miocene to recent vertical motions in the Cretan segment of the Hellenic arc. *Tectonophysics, 234*, 53–72.

Nijholt, N., & Govers, R. (2015). The role of passive margins on the evolution of Subduction-Transform Edge Propagators (STEPs). *Journal of Geophysical Research: Solid Earth, 120*, 7203–7230. https://doi.org/10.1002/2015JB012202

Oertel, G. (1965). The mechanism of faulting in clay experiments. *Tectonophysics 2*, 343-393.

Oberhänsli, R., Candan, O., Dora, O. Ö. & Dürr, S. (1997). Eclogites within the Menderes Massif/ western Turkey. *Lithos 41*, 135-150. https://doi.org/10.1016/S0024-4937(97)82009-9

Okay, A. I. & Tüysüz, O. (1999). Tethyan sutures of northern Turkey. In Durand, B., Jolivet, L., Horvath, F., Séranne, M. (Eds.), *The Mediterranean Basins: Tertiary Extension Within the Alpine Orogen: Special Publications. Geological Society, London*, pp. 475–515.

Okay, A. İ & Satır, M. (2000). Coeval plutonism and metamorphism in a latest Oligocene metamorphic core complex in northwest Turkey. *Geological Magazine, 137*, 495–516.

Okay, A. I, Satır, M., Zattin, M., Cavazza, W. & Topuz, G. (2008). An Oligocene ductile strike-slip shear zone: the Uludağ Massif, northwestern Turkey-Implications for the westward translation of Anatolia. *Bulletin of the Geological Society of America, 120*, 893-911.

Önalan, M. (1997). *Çökelmenin Fiziksel ilkeleri Fasiyes Analizleri ve Karasal Çökelme Ortamları*, İkinci baskı. İstanbul Üniversitesi Basımevi ve Film Merkezi, , İstanbul/Türkiye

Öner, Z. & Dilek, Y. (2011). Supradetachment basin evolution during continental extension: The Aegean province of western Anatolia, Turkey. *GSA Bulletin 123*, 2115-2141. https://doi.org/10.1130/B30468.1

Öner, Z. & Dilek, Y. (2013). Fault kinematics in Supradetachment basin formation, Menderes core complex of western Turkey. Tectonophysics 608, 1394–1412. https://doi.org/10.1016/j.tecto.2013.06.003

Özsayın, E. & Dirik, K. (2007). Quaternary activity of the Cihanbeyli and Yeniceoba fault zones: İnönü-Eskişehir fault system, Central Anatolia. *Turkish Journal of Earth Sciences, 16*, 471-492.

Paton, S. (1992). *The relationship between extension and volcanism in western Turkey, the Aegean Sea and central Greece* [PhD Thesis]. Cambridge University, Cambridge, UK.

Philippon, M., Brun, J.P. & Gueydan, F. (2012). Deciphering subduction from exhumation in the segmented Cycladic Blueschist Unit (Central Aegean, Greece). *Tectonophysics*, 524–525, 116–134. https://doi.org/10.1016/j.tecto.2011.12.025

Platevoet, B., Scaillet, S., Guillou, H., Blamart, D., Nomade, S., Massault, M., Poisson, A., Elitok, O., Özgür, N., Yağmurlu, F. & Yılmaz, K. (2008). Pleistocene eruptive chronology of the Gölcük volcano, Isparta Angle, Turkey. *Quaternaire 19*, 147–156.

Purvis, M. & Robertson, A. (2005). Sedimentation of the Neogene-Recent Alaşehir (Gediz) continental graben system used to test alternative tectonic models for western (Aegean) Turkey. *Sedimentary Geology, 173*, 373–408. https://doi.org/10.1016/j.sedgeo.2003.08.005

Renaut, R.W. & Ashley, G.M. (2002). *Sedimentation in Continental Rifts*. SEPM (Society for Sedimentary Geology) Special Publication, 73, Tulsa, Oklahoma, U.S.A.

Ring, U., Laws, S. & Bernet, M. (1999). Structural analysis of a complex nappe sequence and late orogenic basins from the Aegean Island of Samos, Greece. *Journal of Structural Geology, 21*, 1575-1601. https://doi.org/10.1016/S0191-8141(99)00108-X

Ring, U., Johnson, C., Hetzel, R. & Gessner, K. (2003). Tectonic denudation of a Late Cretaceous–Tertiary collisional belt: regionally symmetric cooling patterns and their relation to extensional faults in the Anatolide belt of western Turkey. *Geological Magazine, 140*, 421-441. https://doi.org/10.1017/S0016756803007878

Rojay, B., Toprak, V., Demirci, C. & Süzen, L. (2005). Plio–Quaternary evolution of the Küçük Menderes Graben (Southwestern Anatolia, Turkey). *Geodinamica Acta, 18*, 317–331.

Sarıca, N. (2000). The Plio-Pleistocene age of Büyük Menderes and Gediz grabens and their tectonic significance on N-S extensional tectonics in West Anatolia: mammalian evidence from the continental deposits. *Geological Journal, 35*, 1-24. https://doi.org/10.1002/(SICI)1099-1034(200001/03)35:1<1::AID-GJ834>3.0.CO;2-A

Seyitoğlu, G. (1999). Discussion on evidence from the Gediz Graben for episodic two-stage extension in western Turkey. *Journal of the Geological Society London, 156*, 1240-1242. https://doi.org/10.1144/gsjgs.156.6.1240

Seyitoğlu, G. & Scott, B. C. (1996). Age of the Alaşehir graben (west Turkey) and its tectonic implications. *Geological Journal, 31*(1), 1–11. https://doi.org/10.1002/(SICI)1099-1034(199603)31:1%3C1::AID-GJ688%3E3.0.CO;2-S

Seyitoğlu, G., Çemen, İ. & Tekeli, O. (2000). Extensional folding in the Alaşehir (Gediz) graben, western Turkey. *Journal of the Geological Society London, 157*, 1097-1100. https://doi.org/10.1144/jgs.157.6.1097

Seyitoğlu, G., Tekeli, O., Çemen, İ., Şen, Ş. & Işık, V. (2002). The role of flexural rotation/rolling hinge model in the tectonic evolution of the Alaşehir Graben, western Turkey. *Geology Magazine 139*, 15-26. https://doi.org/10.1017/S0016756801005969

Seyitoğlu, G., Işık, V. & Çemen, İ. (2004). Complete Tertiary exhumation history of the Menderes Massif, western Turkey: an alternative working hypothesis. *Terra Nova 16*, 358–363.

Seyitoğlu, G., Işık, V. & Esat, K. (2014). A 3D model for the formation of Turtleback surfaces: The Horzum Turtleback of Western Turkey as a case study. *Turkish Journal of Earth Sciences, 23*, 479-494. https://doi.org/10.3906/yer-1401-23

Seyitoğlu, G. & Işık, V. (2015). Late Cenozoic extensional tectonics in western Anatolia: Exhumation of the Menderes core complex and formation of related basins. *Bulletin of the Mineral Research and Exploration, 151*, 49-109 https://doi.org/10.19111/bmre.49951

Smith, N.D. & Perez-Arlucea, M. (1994). Fine-grained splay deposition in the avulsion belt of the lower Saskatchewan River, Canada. *Journal of Sedimentary Research, B64*, 159-168.

Soder, C., Altherr, R. & Romer, R. L. (2016). Mantle metasomatism at the edge of a retreating subduction zone: Late Miocene lamprophyres from the island of Kos, Greece. *Journal of Petrology 57*(9), 1705–1728. https://doi.org/10.1093/petrology/egw054

Şen, F. (2004). *Karadut ve çevresinde Gediz grabeni' nin stratigrafisi ve yapısı* [B.Sc. thesis]. İstanbul, İstanbul University, (in Turkish), 110 pp.

Şen, F. (2016). Late Miocene termination of tectonic activity on the detachment in the Alaşehir Rift, Western Anatolia: Depositional records of the Göbekli Formation and high-angle cross-cutting faults. *EGU General Assembly, 18*, 3541

Şen, F. (2020). Middle Eocene high-K acidic volcanism in the Princes' Islands (İstanbul) and its geodynamic implications. *Turkish Journal of Earth Sciences, 29*(SI-1), Article 9, 208-219. https://doi.org/10.3906/yer-1905-19

Şen, Ş. & Seyitoğlu, G. (2009). Magnetostratigraphy of early–middle Miocene deposits from east–west trending Alaşehir and Büyük Menderes grabens in western Turkey, and its tectonic implications. *Geological Society of London Special Publication, 311*, 321–342. https://doi.org/10.1144/SP311.13

Şen, F. & Ağırbaş, H. (2012). Fold geometry in Karadut fault, Alaşehir graben, Western Anatolia. *International Earth Science Colloquium on the Aegean Region, Proceedings*, İzmir, Turkey, pp: 31.

Şen, F., Karaağaç, S. & Erbil, Ü. (2024). Evidence for High-Angle Origin of the Alaşehir Detachment Fault and Layer-Parallel Shortening During Miocene Time in Alaşehir Graben, Western Anatolia. *Türkiye Jeoloji Bülteni, 67*(1), 17-50. https://doi.org/10.25288/tjb.1318465

Şengör, A.M.C., Tüysüz, O., İmren, C., Sakınç, M., Eyidoğan, H., Görür, N., Le Pichon, X. & Rangin, C. (2005). The North Anatolian Fault: a new look. *Annual Review of Earth and Planetary Sciences 33*, 37–112. http://dx.doi.org/10.1146/annurev.earth.32.101802.120415

Şengör, A. M. C. & Bozkurt, E. (2012). Layer-parallel shortening and related structures in zones undergoing active regional horizontal extension.

International Journal of Earth Sciences, 102, 101-119. https://doi.org/10.1007/s00531-012-0777-0

Thomson, S.N. & Ring, U. (2006). Thermochronologic evaluation of postcollision extension in the Anatolide orogen, western Turkey. *Tectonics, 25*(3), Article TC3005. https://doi.org/10.1029/2005TC001833

Uzel, B., Langereis, C. G., Kaymakçı, N., Sözbilir, H., Özkaymak, Ç. & Özkaptan, M. (2015). Paleomagnetic evidence for an inverse rotation history of Western Anatolia during the exhumation of Menderes core complex. *Earth and Planetary Science Letters, 414*, 108-125. https://doi.org/10.1016/j.epsl.2015.01.008

van Hinsbergen, D. J. J., Langereis, C. G. & Meulenkamp, J. E. (2005). *Revision of the timing, magnitude and distribution of Neogene rotations in the western Aegean region*. Tectonophysics 396, 1–34.

van Hinsbergen, D. J. J., Dekkers, M. J., Bozkurt, E. & Koopman, M. (2010). Exhumation with a twist: Paleomagnetic constraints on the evolution of the Menderes metamorphic core complex, western Turkey: *Tectonics, 29,* Article TC3009. https://doi.org/10.1029/2009TC002596

Wawrzenitz, N. & Krohe, A. (1998). Exhumation and doming of the Thasos metamorphic core complex (S Rhodope, Greece): structural and geochronological constraints. *Tectonophysics 285*, 301–332.

Willis, B. J. & Behrensmeyer, A. K. (1994). Architecture of Miocene overbank deposits in northern Pakistan. *Journal of Sedimentary Research*, B64, 60-67.

Wölfler, A., Glotzbach, C., Heineke, C., Nilius, N.P., Hetzel, R., Hampel, A., Akal, C., Dunkl, I. & Christl, M. (2017). Late Cenozoic cooling history of the central Menderes Massif: Timing of the Büyük Menderes detachment and the relative contribution of normal faulting and erosion to rock exhDumation. *Tectonophysics 717*, 585–598. https://doi.org/10.1016/J.TECTO.2017.07.004

Wright, D.T. (1999). The role of sulphate-reducing bacteria and cyanobacteria in dolomite formation in distal ephemeral lakes of the Coorong region, South Australia. *Sedimentary Geology, 126*(1–4), 147–157. https://doi.org/10.1016/S0037-0738(99)00037-8

Yang, X. B., Wang, H. Y., Li, Z. Y., Guan, C. & Wang, X. (2021). Tectonic-sedimentary evolution of a continental rift basin: A case study of the Early Cretaceous Changling and Lishu fault depressions, southern Songliao Basin, China. *Marine and Petroleum Geology, 128*, Article 105068. https://doi.org/10.1016/j.marpetgeo.2021.105068

Yılmaz, Y., Genç, Ş.C., Gürer, Ö.F., Bozcu, M., Yılmaz, K., Karacık, Z., Altunkaynak, Ş. & Elmas, A. (2000). When did western Anatolian grabens begin to develop?. *Geological Society of London Special Publication, 173*, 353-384. https://doi.org/10.1144/GSL.SP.2000.173.01.17

Yılmaz, Y. (2017). Major Problems of Western Anatolian Geology. Çemen, İ. & Yılmaz, Y. (Eds.), *Active Global Seismology: Neotectonics and Earthquake Potential of the Eastern Mediterranean Region, Book Series, Geophysical Monograph Book Series, 225*, 141-187. https://doi.org/10.1002/9781118944998.ch6

Yuretich, R.F. & Ervin, C.R. (2002). Clay minerals as palaeoenvironmental indicators in two large lakes of the African Rift Valleys: Lake Malawi and Lake Turkana. In Renaut, R. W. & Ashley, G.M. (Eds.), *Sedimentation in Continental Rifts: SEPM (Society for Sedimentary Geology) Special Publication 73*, 221–232, https://doi.org/10.2110/pec.02.73.0221